Comparison Between Thermophilic and Mesophilic Membrane-Aerated Biofilm Reactors- A Modeling Study

By

DUOWEI LU

A thesis submitted to the faculty of graduate students

Lakehead University

In partial fulfillment of the requirement for the degree of

Master of Science in Engineering

Environmental engineering

Lakehead University

Table of Contents

List of tables and graphs

Acknowledgements

Foremost, I would like to express my sincere gratitude to my advisor Dr. Baoqiang Liao and Dr. Hao Bai for the support of my master study and research, for their patience, motivation, enthusiasm, and immense knowledge. Their guidance helped me in all the time of research and writing of this thesis.

Besides my advisors, I would like to thank the rest of my thesis committee: Dr. Siamak Elyasi, Dr. Amir H. Azimi, for their encouragement and insightful comments.

I thank my fellow labmates in Lakehead University: Yichen Liao, Lishan Yao for the stimulating discussions, for the sleepless nights we were working together before deadlines, and for all the fun we have had in the last two years. Also I thank my friends: Minoo Ataie, Sepher Kenjur

Last but not the least, I would like to thank my family: my parents Xingxiao Ying and Jinzhao Lu for giving birth to me at the first place and supporting me spiritually throughout my life.

Abstract

Membrane aerated biofilm reactor (MABR), as a novel biological waste treatment technology, has received much attention in recent years, due to its advantages, as compared to conventional biofilm. Considerable amount of research and development of MABR technology were conducted in lab-scale, pilot-scale studies and even full-scale applications for various types of waste treatment and air pollution control. Though many researches have mentioned that operation factors would result in different system performance, few researches are focused on temperature changing impacts. While thermophilic aerated biological treatment already became a hot issue for waste water treatment. Thus, combined with thermophilic aerated biological treatment, the concept of thermophilic membrane-aerated biofilm reactor (ThMABR) is proposed in this research. This concept has a great potential to develop a new type of ultra-compact, highly efficient bioreactor for high strength wastewater. In order to prove the high temperature has positive effect on MABR system, a mathematic modeling was established. Mathematical modeling was conducted to investigate the impact of temperature (mesophilic vs. thermophilic) on oxygen and substrate concentration profiles, membrane-biofilm interfacial oxygen concentration, oxygen penetration distance, and oxygen and substrate fluxes into biofilms.

In the first part of this thesis, it focuses on a state-of-the-art literature review (2007-present) on the research progress and technology development of the MABR technology. The biological and membrane performances of MABRs for chemical oxygen demand (COD) and nitrogen removal in wastewaters, air pollution control, and modeling studies are systematically reviewed and discussed. However, few articles mentioned the temperature changing effect on MABR system.

So in the second part, the concept of thermophilic membrane-aerated biofilm reactor (ThMABR) is proposed. This concept combines the advantages and overcomes the disadvantages of conventional MABR and thermophilic aerobic biological treatment, and has a great potential to develop a new type of ultra-compact, highly efficient bioreactor for high strength wastewater and waste gas treatments. Mathematical modeling was conducted to investigate the impact of temperature (mesophilic vs. thermophilic) on oxygen and substrate concentration profiles, membrane-biofilm interfacial oxygen concentration, oxygen penetration distance, and oxygen and substrate fluxes into biofilms. The general trend of oxygen transfer and substrate flux into biofilm between ThMABR and MMABR was verified by the experimental results in the literature. The results from modeling studies indicate that the ThMABR has significant advantages over the conventional mesophilic MABR in terms of improved oxygen and pollutant flux into biofilms and biodegradation rates and an optimal biofilm thickness exists for maximum oxygen and substrate fluxes into biofilm.

Key words: Membrane-aerated biofilm reactor; thermophilic membrane-aerated biofilm reactor; mesophilic membrane-aerated biofilm reactor; comparison; modeling.

1. Introduction

Wastewater pollution has been a significant challenge to modern society. Every day, more than two million tons of human wastes are discharged into the waterbody; more than 70% of industrial wastes are dumped untreated into waters where they pollute the usable water supply in developing countries; and more than 1.2 billion people are lack access of safe drinking water (Shannon et al., 2008). Thus, it is highly desirable to develop innovative technologies for wastewater treatment and management. Significant progress has been made in developing novel and efficient wastewater treatment technologies (Shannon et al., 2008). Among these novel technologies, membrane aerated biofilm reactor (MABR) is a relatively new technology with distinct advantages, including high removal efficiency, simultaneous COD and N removal, high oxygen transfer rate and utilization, high energy efficiency, minimum stripping of volatile organic compounds, easy to operate at high solids retention times, and compactness, as compared to conventional biofilm and suspended growth technologies, for wastewater treatment (Meyer, 2015).

The MABR as a new emerging technology has been proposed as a promising alternative to the conventional biofilm reactors for aerobic wastewater treatment. This technology offers unique advantages over conventional biofilms such as specialized treatment (Martin and Nerenberg, 2012; Wei et al., 2016) and high energy efficiency (Liao and Liss, 2007). A variety of approaches has been successfully tried under both thermophilic and mesophilic testing conditions (Liao and Liss, 2007). The use of gas permeable membrane can achieve bubble-free aeration and consequently 100% utilization of the oxygen. This novel design represents a very high energy efficiency compared to the conventional aerobic biological treatment processes. In the activated sludge processes, only 10-20% oxygen utilization can be accomplished and aeration

account for approximately 73% of the operating cost. In MABR system, due to the permeable hollow fiber membranes are adapted as platform for the attachment of biofilm, the bubbleless oxygen can transfer in a high efficiency (Li and Zhang, 2018).

The MABR system utilizes hydrophobic membranes to immobilize biofilms on the outside of membrane which can offer molecular oxygen directly from the inner part to the biofilm. Hydrophobic gas-permeable membranes will be used as a carrier of biofilm and for less bubble oxygen transfer. Due to the counter-diffusion concept, oxygen can be offered to the bottom of the biofilm and the substrates such as ammonia and carbon are provided from the bulk liquid phase. Thus, the energy efficiency of the MABR system is much higher than that of the activated sludge processes. Figure 1 shows the structure of MABR system. Compared with conventional biofilm reactors, there is a new symbiotic environment for microorganism communities for nutrients removal. The substrate diffuses inversely which can lead a larger active thickness in biofilm than conventional biofilm systems, which has a co-current diffusion of both oxygen and substrate.

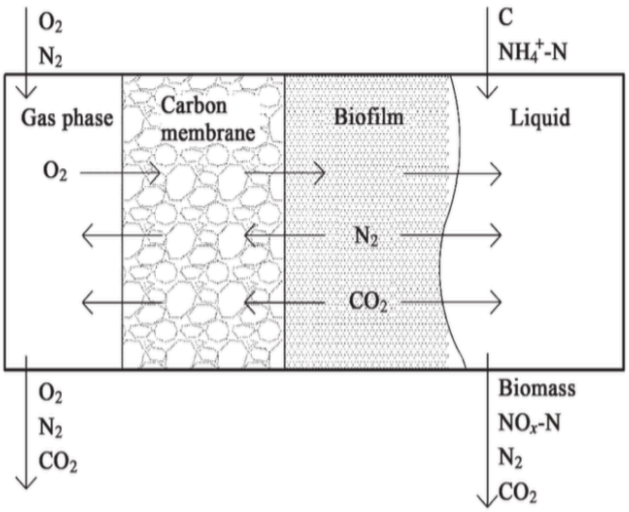

Figure 1. Schematic diagram of the MABR (drawn after Casey *et al.*, 1999).

Due to the unique counter-diffusion of oxygen and substrate in an MABR biofilm, aerobic zone and an anaerobic/or anoxic zone of biofilm co-exist and thus can achieve simultaneous nitrification and denitrification for nutrients removal, in addition to COD removal. The microbial population stratification is useful for simultaneous removal of nitrogen existing in an MABR system. The concentration of oxygen is the highest at the biofilm-membrane interface decreasing toward the bulk liquid phase where the nutrient concentrations are the highest at the biofilm and water interface. This stratification and adequate biofilm thickness maintenance can be used to simulate the biochemical oxygen demand and nitrogen removal in one tank. Besides that, the active aerobic biofilm region is near the membrane where the oxygen is plentiful. The bacteria can reduce some degree of the effect of toxic chemicals which may inhibit microorganism community growth.

The interest of research in MABR is its low energy requirement. According to research (Ahmed et al., 2004), membrane Oxygen Transfer Efficiencies (OTEs) can be reached to 100% and this process will not be sensitive to affect the size and residence time of bubbles. Less air/oxygen is required in MABR, and it can reduce the blower volumetric flow rate and the operating pressure because of the higher OTEs. It provided a chance for saving operation cost and increase the lifetime of a plant for waste water treatment (Iorhemen et al., 2017).

Some experts (Syron and Casey, 2008) had explored and summarized the basic understanding of the MABR process (biofilm characteristics, membrane performance, and mass transfer), key parameters for operation, future development and the limitations of the current process. MABR has an excellent performance in a high concentration of ammonium waste water treatment because of the slow growth of nitrifying bacteria in the biofilm with the direct supplication of

oxygen to biofilm (Feng et al., 2007). Research and development of the MABR technology has become one of the hot topics for wastewater treatment (Syron and Casey, 2008).

The other emerging technology for waste abatement is the thermophilic aerobic biological treatment (TABT) process. It is a unique and relatively new process characterized by rapid biodegradation rates, low sludge yields, and excellent process stability (LaPara et al., 2000). Under thermophilic conditions (45-65^{o}C), substrate utilization rates are 3-10 times higher than those observed in mesophilic processes (25-35^{o}C) and the sludge yield is similar to that of anaerobic processes (LaPara et al., 1999). These advantages have made Thermophilic MABR (ThMABR) extremely suitable for the treatment of high strength industrial wastewater, such as pulp and paper mill effluent and food processing wastewater. However, low oxygen solubility combined with the high oxygen transfer rate required to sustain rapid biodegradation make the selection of aeration equipment one of the most critical process design choices at thermophilic temperatures (Duncan, et al., 2017). In addition, poor flocculation potential and foaming problem of thermophilic bacteria represent other unique challenges for biomass separation in the suspended growth process.

In this paper, biological performance, membrane performance, and modelling studies of MABR are systematically reviewed. The concept of ThMABR technology is proposed and studied by theoretical analyses and modeling. Coupling the advantages of conventional MMABR technology with ThMABR overcomes their disadvantages and represents an innovative approach to the treatment of high strength industrial wastewater and waste gases. On the one hand, the gas permeable membrane is the ideal aeration equipment for the delivery of the high rate oxygen transfer required for rapid biodegradation in the ThMABR process; such rates are not achievable with conventional aeration technologies. On the other hand, the low yield and dispersing growth

nature of thermophilic microorganisms represent a unique strategy for controlling excessive growth of biofilms on the gas permeable membrane. In addition, thermophilic treatment increases the penetration distance of oxygen, pollutants and nutrients in biofilms significantly due to increased diffusivities and decreased viscosities at thermophilic temperatures. It is anticipated that an ultra-compact, highly efficient bioreactor will be developed for high strength wastewater and waste gas treatment through the ThMABR concept.

This communication presents theoretical analyses and modeling results of MMABRs. Of particular interest are the differences between ThMABRs and MMABRs in terms of oxygen and pollutant flux and penetration distances, biodegradation rate, biofilm growth and detachment.

2. Literature review

2.1 Biological performance of MABR

2.1.1 Effect of operation conditions on COD/BOD removal

The operating conditions play an important role in controlling the COD removal efficiency. To achieve a better COD removal efficiency, identification of the optimal operating conditions is essential. Because the conventional biofilms are thick, it will lead to only fraction of dissolved oxygen penetration into a biofilm. The MABR system with optimal operation conditions can achieve the complete utilization of oxygen and biofilm in wastewater treatment.

Table 1 showed the advanced studies on COD removal in MABR systems from 2007 to 2017. These studies demonstrated excellent abilities of MABRs for COD removal (50-93%) compared with 64% COD removal rate in conventional activated sludge process (Tong et al., 2013), depending on the types of wastewater treated and operating conditions, and optimal conditions of MABRs were identified.

Table 1 The biological performance of MABR on COD removal

Type of waste water	HRT	pH	Aeration pressure	Temperature	Removal efficiency	Ref
Synthetic waste water containing PCE	9-48 h	/	/	/	COD 85-93 %	Ohandja and Stuckey 2007
Oil-field Waste water	8-12 h	/	0.1 M-0.2 M	/	COD 82.3 %	Li et al., 2015
Synthetic waste water	12 h	7.8-8.4	0.1-0.2 M	20±2 ℃	COD 60.9 %-80 %	Xin et al., 2012
Industrial wastewater	39-50 h	/	0.1 M	/	COD 90.2 %	Xin et al., 2012
Synthetic wastewater	8-20 h	/	/	32±1 ℃	COD 86%-87.5 %	Hu et al., 2008
Synthetic wastewater	8-16 h	/	0.01-0.015 M	30±2 ℃	COD 90±2 %	Liu et al., 2007
High strength synthetic wastewater	/	6.8-6.9	4 or 6psi	55 ℃	COD 90 %	Liao and Liss, 2007
Synthetic wastewater	/	/	/	28±1 ℃	COD 83.5 %	Hu et al., 2009
Urban river	15 h	8.0	0.30 M	19 ℃	COD 87 %	Li et al., 2016
High-concentration pharmaceutical intermediate wastewater	24 h	/	0.15 M	15.0±0.1 ℃	COD 95 %	Tian et al., 2015
Surface water	/	/	/	/	COD 37.5 %	Li et al., 2016
Synthetic wastewater	12 h	/	0.005 M or 0.01 M	40 ℃	COD 85.9 %	Hou et al., 2013
Synthetic wastewater	/	7.5-8	0.025 M	30±2 ℃	COD 85%	Liu et al., 2010

Li et al., (2015) investigated the effect of aeration pressure (0.1-0.2 MPa) in MABR on COD removal and found out that an optimal aeration pressure of 0.15 MPa could achieve the effluent COD removal of 95mg/L. At the beginning, the 0.2 MPa aeration pressure gave the highest COD removal, but with experimental going on, the 0.15 MPa aeration pressure achieved the lowest effluent COD. The main reason could be the fact that other organic matters in influent were degraded to short chains by hydrolysis acidification and aerobic oxidation. Similarly, Hou et al., (2013) conducted an aeration pressure experiment to find the optimal aeration pressure for COD removal in an MABR. The COD removal rates at 0.01 MPa and 0.02 MPa of aeration pressure were obviously higher than at 0.005 MPa. The effluent COD concentration was below 20 mg/L and the removal efficiency attained 90% after 1h of operation when the aeration pressure is 0.01 MPa. Finding the optimal aeration pressure is very important for us to use the MABR systems

for COD removal. However, the effect of oxygen concentration should be considered when controlling aeration pressure. The oxygen concentration will also affect the COD removal efficiency. If pure oxygen instead of air was used to treat a synthetic wastewater, it could improve the COD removal efficiency under the same operating conditions in mesophilic MABR system (Zheng and Liao, 2016). However, this phenomenon was not significant in thermophilic MABR system (Zheng and Liao, 2016). The reason might be related to the increased water vapor at the thermophilic temperature. A higher temperature (thermophilic) would increase the water vapor into the cavity of the hollow fiber membrane, thereby increasing the water vapor pressure and possibly water vapor condensate in the hollow fiber membrane (Zheng and Liao, 2014). The water vapor in the membrane chamber would increase the oxygen mass transfer resistance, thereby reducing the oxygen transfer rate at the thermophilic temperature. Although the oxygen concentration can enhance the removal efficiency at a certain level, but a continued increase in the oxygen concentration might decrease the performance of MABR. For example, the pure oxygen inhibited the removal efficiency of COD (Liu et al., 2007). In this experiment pure oxygen was used to study its effect on the biological performance of MABR. The effluent COD concentration increased above 100 mg/L. The main reason for this phenomenon was that the microbial community structure become loose within the biofilm and oxygen toxicity when the oxygen partial pressure became high (Liu et al., 2007).

Hydrodynamic condition is another important factor affecting COD removal in MABR process. It has been proved that hydrodynamic condition can affect the biofilm density, porosity and the thickness of the concentration boundary layer at the biofilm-liquid interface, the mixing of bulk liquid, and the bacterial activity and community structure (Syron and Casey, 2008). Xin et al., (2012) conducted a series of experiment to investigate the effect of flow velocity on COD

removal. It was found that when the feed flow velocity increased from 0.01 m/s to 0.05 m/s, the effluent concentration of COD decreased significantly. The impellers can increase the flow rate under the plug-flow pattern in MABR system. Due to this enhanced velocity, it promoted mass transfer inside the biofilm, which avoided the excessive microbial growth which has a positive effect on COD removal (Li et al., 2016). Hu et al., (2016) also pointed out the MABR system became more effective on COD removal with increasing the flow velocity. It stated that higher flow velocity has a contribution on aggregations and bio-sorption of COD. From the above studies, it is clear that the higher flow velocity enhanced the system performance. The kinetic energy could wake up the microbial activity because it can change the biofilm density and microbial community structure. Theoretically, the flow rate immediately below the biofilm / liquid interface is negligible. The negligible flow area is called the hydrodynamic boundary layer. Its thickness depends on the linear velocity which means the higher the velocity will lead the thinner the boundary layer. The area outside the boundary layer is characterized by significant mixing or turbulence. For fluid states characterized by laminar turbulence, the hydrodynamic boundary layer may substantially affect cell-matrix interactions. The cells behave as particles in the liquid, and the sedimentation rate and the correlation with the immersion surface will depend to a large extent on the velocity characteristics of the liquid. At very low linear velocities, the cells must pass through a fairly large hydrodynamic boundary layer, and the association with the surface will depend to a large extent on cell size and cell motility.

Other operation conditions also affect COD removal. The COD value of effluent in MABRs decreased with increasing the Hydraulic Retention Time (HRT) (Hu et al., 2016). The COD removal efficiency would increase with an increase in influent pH value (<8.0) then decrease with a further pH increase (pH>8). Zheng and Liao (2016) investigated the effect of HRT on

COD removal efficiency in thermophilic and mesophilic MABR systems. The results showed that with increasing the cycle length time, the COD removal efficiency increased from 56±6 % to 68±3 % (thermophilic MABR) and 61±5 % to 72±2 % (mesophilic MABR), respectively. Besides that, the variation of pH value could affect removal efficiency of COD (Li et al., 2016). Different operation conditions led different biological performance. Thus, optimization of process conditions provides tremendous opportunities in research for the MABR systems. We can rely on the information to adjust operation conditions to achieve the maximum COD removal efficiency or system abilities.

2.1.2 Effect of operation conditions on nutrient removal

Nutrient removal is one of the main concerns in modern wastewater treatment especially in some areas which are sensitive to eutrophication. Currently, the most widely applied technology for N-removal from municipal wastewater is nitrification combined with denitrification. Phosphorus precipitation and biological phosphorus removal can be implemented in MABR system. Ammonia, nitrate, and nitrite can be changed to nitrogen by microbial bacteria. MABR is particularly suitable for simultaneous COD and nutrients (N and P) removal, due to the co-exist of aerobic, anoxic and anaerobic zones in biofilms attached on membrane surfaces.

Recently MABR systems have demonstrated excellent nutrient removal efficiency. Table 2 displayed the research results from 2007 to present about the biological performance of MABR system for nutrients removal. The N and P removal efficiency was in the range of 50-90 % and 85 %, respectively (Table 2) is much than activated sludge system (District et al., 2009).

Table 2 The biological performance of MABR on nutrient removal

Type of waste water	HRT	pH	Oxygen partial pressure	Temperature	Influent concentration	Removal efficiency	Ref
Synthetic waste water	85-260min	6.7-7.9	0.21-0.6atm	23±2℃	20-35 mg NH_4^+-NL^{-1}	> 90%	Motlagh 2008
Synthetic Waste water contains PhACs	0.96-9.6d	/	/	28±1℃	500 mg NL^{-1} PhACs 15 μgL^{-1}	TN> 80% PhACs> 80%	Lai et al., 2015
Synthetic waste water	/	7.5±0.2	/	28±1℃	80 mg/L NH_4^+-N	83.5%	Hu et al., 2009
Synthetic wastewater	12 h	7.8-8.3	0.15 MPa/0.10 MPa	20±2℃	60-70 mg/L NH_4^+-N 9-13 mg/LTP	NH_4^+-N 96% TN 91% TP 85%	Sun et al., 2015
Synthetic wastewater	3.6d	/	/	/	30 mg/L NH_4^+-N	Ammonia 96% Nitrogen 52%	Yu et al., 2011
Synthetic municipal wastewater	/	/	170 kPa	28-33℃	NH_4 Cl, 15000 mg/L	When DO is 0.5 mg/L, Ammonia 96% TN 65.7% DO is 1.05 mg/L TN 78.4%	Dong et al., 2009
Artificial wastewater	24h	7.0-8.0	0.025 MPa	20±2℃	NH_4^+-N 70 mg/L	NH_4^+-N 55.67 kg/m^3d Specific TN 52.87 kg/m^3d	Lin et al., 2015
Leachate	5-7.5d	7.5-8.0	/	21-27℃	Ammonium	Ammonia 90%	Syron, 2015
Acetonitrile Wastewater	30h	/	/	/	Acetonitrile 0.332-1.393 g/L	Acetonitrile 96.7±3.14%	Li et al., 2008
Synthetic wastewater	/	6.71-8.31	10±5 kPa	26℃	L_{NH4} =1.3±5 g N/L/day	72%	Pellicer-Nàcher et al., 2010
High-Strength Industrial Sewage	/	/	/	/	L_{TKN}=0.103 g N/m^2 d	94%	Stricker et al., 2011
Synthetic wastewater	0.8d	7.2±0.2	/	30±1℃	200 g-NH_4^+-N/m^3	R1 46.6% R2 47.2%	Lackner et al., 2010
Synthetic wastewater	6h	7.9	0.015 MPa-0.04 MPa	35℃	200 mg-NH_4^+-N/m^3	77%	Gong et al., 2007
Synthetic wastewater	5-8h	7.5	/	25℃	400-850 mg/L NH_4^+-N	90%	Cao et al., 2009

MABR systems have excellence performances on nutrient removal. Controlling the operation conditions is essential for achieving better performance. If DO concentration of MABR system was decreased to 0.5mg/L, the total nitrogen removal efficiency increased to 24%, however, the ammonia removal efficiency dropped to 86% (Yu et al., 2011). Furthermore, Dong et al., (2009) used a membrane aeration/filtration combined bioreactor to study the effect of DO level on nutrient removal. They found that the ammonia removal efficiency increased with an increase in the DO concentration but the nitrification was still inhibited by oxygen limitation when the DO

concentration was 0.1 mg/L. The Total Nitrogen (TN) removal was also greatly affected by the DO concentration. When the DO concentration was increased from 0.1mg/L to 0.5mg/L, the TN removal efficiency was enhanced by 12.7%. However, if DO concentration kept rising, the TN removal efficiency decreased sharply. It dropped to 50% and 26% when the DO concentration was 2mg/L and 4mg/L, respectively (Dong et al., 2009). Feng et al., (2008) employed an MABR to investigate the effects of aeration on nutrients removal and to identify the dominant bacterial community of the biofilm for partial nitrification. The attached nitrifying biofilms included both Ammonia-oxidizing Bacteria (AOB) and Nitrite-oxidizing Bacteria (NOB) community which utilized diffused air. Most of the DO in the permeate membrane was effectively consumed by the biofilm, and only a small amount was released to the bulk phase, which resulted in an anoxic state associated with DO levels below 0.6 mg/L. The low DO level was insufficient for complete nitrification made the system very suitable for performing subsequent ANAMMOX processes (Feng et al., 2008). The TN removal efficiency also increased with an increase in the DO level at a certain range (0.7-1.4mg/L). If DO level surpasses this range, it will cause the limitation for microbial activity which reduces the nutrients removal efficiency (Feng et al., 2008). Therefore, the DO level should be set, based on the microbial community demand, to get the optimal performance for nutrients removal.

The nutrient removal efficiency might also be affected by both wastewater COD/BOD concentration and composition. Downing and Nerenberg (2008) found out that the bulk liquid biological oxygen demand (BOD) concentrations would affect the nitrifying and denitrifying function of the MABR system. When the concentration of bulk liquid BOD was 3 and 10 mg/L, the nitrifying rate decreased to 1 and 0.4 g N /m^2d, respectively. However, an increase of the BOD concentration from 1 to 10 g/m^3, the denitrification efficiency was increased from 20% to

100% (Downing and Nerenberg, 2008). A change in the wastewater composition would also impact the MABRs performance. If changed COD/TN ratio increased from 3 to 7, the TN removal efficiency in SBMABR would be increased from 55% to 91% (Sun et al., 2015). Besides that, the Total Phosphorus (TP) removal efficiency in Sequencing Batch Membrane-aerated Biofilm Reactor (SBMABR) system is improved as well with the increase of COD/TP ratio and finally attained 85%, which was much higher than TP removal efficiency in Carbon Membrane-aerated Biofilm Reactor (CMABR) (Sun et al., 2015). According to these results, it is feasible to improve the MABR system efficiency by changing the ratio of influent pollutants. Besides that, the phenomenon also proved the flexibility of MABR systems (Sun et al., 2015). Although there was little difference in the removal of TN and TP at the sludge retention time (SRT) of 20, 25, 30 and 40 days, the variation in the C/N ratio in feed affected the removal efficiency. When the C/N ratio was 4.5, the TN removal was the highest (80 %) compared with the C/N ratios at 2.0 and 7 (Matsumoto et al.,2007). Furthermore, it was feasible to remove phosphorus when the C/N ratio was at 10, which is suitable for the TP removal bacteria growth (Choi et al., 2008). While the NO_x^--N removal rates corresponded to the change in the C/N ratio. A higher N removal efficiency was achieved at a high C/N ratio (Cao et al., 2009). A higher C/N ratio would provide a larger amount of carbon source for denitrification, resulting in a lower NO_x^--N concentration in the effluent (Cao et al., 2009). However, Matsumoto et al., (2007) found that a high C/N ratio was not suitable for TN removal in MABR system, because a high C/N ratio was more appropriate for heterotrophic bacteria (HB) growth, which would surpass the AOB and NOB growth in the biofilm and thus leads to a decrease in TN removal efficiency (Matsumoto et al., 2007). Thus, the adjustment of the C/N ratio in wastewater could optimize the performance of MABR for biological nutrients removal.

The nitrogen removal would also be affected by influent nutrients loading rate and reactor configuration. Lackner et al., (2008) observed the differences in TN removal between a co-diffusion and a counter-diffusion system. The TN removal efficiency changed with a change in NH_4^+ loadings. At 1.2 g-$Nm^{-2}d^{-1}$ loading, the counter-diffusion system could get 93% removal efficiency and co-diffusion system achieved 91%. However, when the loading rate increased to 4g-$Nm^{-2}d^{-1}$, the removal efficiency decreased to 66% (counter-diffusion) and 36% (co-diffusion). Lin et al., (2015) used a polyvinylidene fluoride (PVDF) membrane-aerated biofilm reactor to study the nitrogen removal performance. When the influent NH_4^+-N concentration was 70mg/L, the NH_4^+-N conversion was above 77.5%, and the TN removal efficiency was around 78.6%. However, a further increase in the influent NH_4^+-N concentration to 100mg/L led to a decrease in the TN removal efficiency (71.6%) (Lin et al., 2015). But, the influent concentration was decreased to 50mg/L again, the TN removal ability recovered quickly. Therefore, there is an optimal NH_4^+-N loading rate that gives the maximum TN removal efficiency in the MABR systems. If the nutrients loading rate surpassed a certain range, the activity of microbial bacteria might be limited.

Other operation conditions, such as pH, could also affect the MABR system performance. The pH changing will affect the kinetics of nitrification. Shanahan and Semmens (2015) found that the bicarbonate alkalinity of the influent had a significant effect on nitrification performance of MABR. The biological nitrification performance increased from 65% to 77% when the bicarbonate concentration increased from 0.6 to 4.8 mM. The operation temperature can perform as a factor to control the MABR system biological performance. Liao et al., (2010) pointed out there was a big difference in nitrogen removal between mesophilic MABR and thermophilic MABR. The mesophilic MABR had a higher removal efficiency than thermophilic MABR

because there was no stable nitrification occurring under the thermophilic conditions.

2.1.3 Air pollution control

2.1.3.1 The mechanism of air pollution control in MABR system

MABR systems can be applied in waste gas treatment, due to the high utilization rate of pollutants in MABR systems. Their lower operating costs, biotechnologies which caused lower chemical consumptions and CO_2 emissions have become the hot spot in air pollution control research (Álvarez-Hornos et al., 2011). MABR can overcome the mass transfer limitations because of its advanced permeability and the affinity of certain membranes for hydrophobic contaminants (Kumar et al., 2008). The air pollutants pass through the membrane to allow contaminants to passively pass through the membrane to the liquid biofilm phase on the other side, driven by a concentration gradient. The mass transfer coefficient through the dense membrane depends on the solubility of the contaminants and the diffusion coefficient (Kumar et al., 2008).

2.1.3.2 Effect of operation conditions on air pollutants removal

Table 3 showed the studies for waste gas treatment in MABR systems science 2008. The operation conditions are sensitivity to microbial communities in a membrane which directly affect the pollutants removal efficiency.

Table 3 The biological performance of MABR for waste gas treatment

Waste gas type	Reaction temperature	GRT	Inlet concentration	Removal efficiency	Ref
Acetone, toluene, Limonene, hexane Mixing gas	23 ℃	60 s,30 s, 15 s,3 s	Acetone 2.5±0.1 mg/m^3 Toluene 2.4±0.1 mg/m^3 Limonene 3.2±0.1 mg/m^3 Hexane 1.3±0.0 mg/m^3	Acetone 93 % Toluene 93 % Limonene 90 % at 7 s GRT Hexane 24 %	Lebrero et al., 2013
Dimethyl sulfide	52 ℃	36 s,24 s,12 s,10 s,8 s	75 ppmv	90 % at 24 s GRT	Luvsanjamba et al.,2008
Ethyl acetate	23 ℃	15 s,30 s,60 s	0.5-4.6 N/m^3	95 % at GRT 15 s	Álvarez-Hornos et al.,2011
Toluene vapors	30±0.5 ℃	2-28 s	1.0 gTOL/m^3	78%-99%	Kumar et al.,2008
Ethyl acetate N-hexane Toluene	23 ℃	15 s,30 s,60 s	Total VOC 500 mgC N/m^3 to 2500 mgC N/m^3	99% ethyl acetate at 15 s GRT toluene 66% at 60 s GRT Low removal efficiency for Hexane	Álvarez-Hornos et al., 2012
Ordor	25 ℃	4-84 s	4.9 ± 0.5 MeSH mg/ m^3 0.82 ± 0.07 toluene mg/ m^3 0.91 ± 0.10 alpha-pinene mg/ m^3 0.75 ± 0.08 hexane mg/ m^3	90%	Lebrero et al., 2014
Trichloroethylene Toluene	30 ℃	4.5-15.7 s	450-2400 mg/m^3 toluene 100-160 mg/m^3 TCE	95% toluene 22.1% TCE	Zhao et al., 2011

Gas residence time (GRT) is a crucial factor affecting the biological performance in MABR systems for air pollution control. Lebrero et al., (2013) installed a flat-membrane biofilm reactor to remove the acetone, toluene, limonene, and hexane from waste gas. During the operation, the MABR system achieved a toluene removal efficiency larger than 99% at GRTs of the 60s and 30s. When the GRTs decreased to 15s and 7s, the toluene removal efficiency dropped to 97±1% and 93±0%, respectively. Similarly, the limonene removal efficiency decreased with reducing the GRTs. The removal efficiency of limonene decreased from 98±1% to 95±1% and 90±1%, respectively, when the GRTs decreased to 15s and 7s. However, the GRTs change did not affect the hexane removal efficiency. Even the GRTs decreased to 30s, 15s, and 7s, the system could still get a steady removal efficiency of hexane (14±3%). Álvarez-Hornos et al., (2011) found out that the increasing of empty bed residence time (EBRT) led to an increase in the ethyl acetate

removal efficiency in an MABR system. When the EBRTs increased from 15s to 60s, the ethyl acetate removal efficiency increased from 45% to 80%. Luvsanjamba et al., (2008) investigated the effect of GRT on the dimethyl sulfide (DMS) removal efficiency. When the GRTs decreased from 24 to 12 and 8s, the DMS removal efficiency was reduced from 76% to 56% and 40%, respectively. The main reason was that the MABR system changed from a reaction rate-controlled to a mass transfer rate-controlled bio-system with a decrease in the GRT. However, when the GRT increased from 24 to 36s, the removal efficiency increased from 76% to 88%. Furthermore, Kumar et al., (2010) investigated toluene vapors removal by a MABR. They found that a higher removal efficiency could be achieved at the same inlet concentration with a longer GRT. And at the same GRTs, a lower inlet toluene vapors concentration will enhance the removal efficiency.

Waste gas degradation efficiency would also change with different inlet pollutant concentrations. Zhao et al., (2011) tested the degradation of toluene at inlet concentration level of 450, 900, 1400, 1800 and 2400 mg/m^3. The removal efficiency was 88% at an inlet pollutant concentration of 450 mg/m^3. When the inlet pollutant concentration was increased to C_{in}=900 and 1400 mg/m^3, the removal efficiency was decreased to 70% at the beginning and then gradually recovered for both cases. However, a further increase of the inlet pollutant concentration to 2400 mg/m^3 led to a decrease in the final removal efficiency at 65%. At the same time, the biofilm performance is sensitive to the variation of pH value. If nutrient solution pH value was below 7 or above 7.5, the removal efficiency of toluene decreased.

When the MABR systems are used to treat waste gas, it is essential to maintain the optimal operating conditions, such as the GRTs, influent gas concentration and others, for a high waste gas removal efficiency. MABR systems have already displayed advanced performance in air

pollution control, as compared to conventional biofilm systems but full applications of MABR systems need further studies.

2.1.4 Microbial community

The unique combination of aerobic, anoxic, and anaerobic zones of biofilms in MABR systems may lead to different microbial communities in each biofilm zone. This is the foundation for nutrients removal (N) (co-exist of nitrification and denitrification zones) in the MABR systems. Consequently, considerable efforts have been paid to understand microbial community in the biofilms of MABR systems.

2.1.4.1 Biological process in MABR systems

The MABR systems own considerable interest because of its advanced design and cost-effective characteristics such as the unique opposite mass transfer of oxygen and nutrients for nutrient removal and large effective surface area of the hollow fiber membrane for microbial community adherence and growth (Tian et al., 2015). Also, the microbial community living in the MABR biofilm is expected to be different from the biofilm produced in conventional reactors. For example, nitrifying bacteria usually grow at the bottom of the biofilm, where the chemical oxygen demand (COD) concentration is low and the oxygen level is high at the membrane-biofilm interface. In contrast, heterotrophic bacteria (such as denitrifying bacteria) grow outside the biofilm, where the COD concentration is high and the oxygen concentration is low at the biofilm bulk water interface (Tian et al., 2015). This system represents an advanced technology for removing contaminants, including nutrients, from wastewater.

In this system, single-stage autotrophic nitrogen removal was achieved by the close cooperation between AOB and Anammox bacteria. When the AOB oxidize ammonia to nitrite, it will consume oxygen. Due to this, it created the anoxic conditions for Anammox bacteria.

$$NH_4^+ + 1.5O_2 \rightarrow NO_2^- + 2H^+ + H_2O \quad (1)$$

Then the Anammox bacteria converted the produced nitrite into dinitrogen gas.

$$NH_4^+ + 1.3NO_2^- \rightarrow 1.02N_2 + 0.26NO_3^- + 2H_2O \quad (2)$$

Oxygen and ammonium concentration gradients cause biofilm layer dividing, where AOB grows near the surface of the membrane, where both oxygen and ammonium are available and biofilm grows near the bulk fluid of ammonium and nitrite phase, which is oxidized by aerobic ammonium (Figure 2). These two microbial processes can be combined in a sufficient thickness for biofilm to produce aerobic and anaerobic conditions in the MABR.

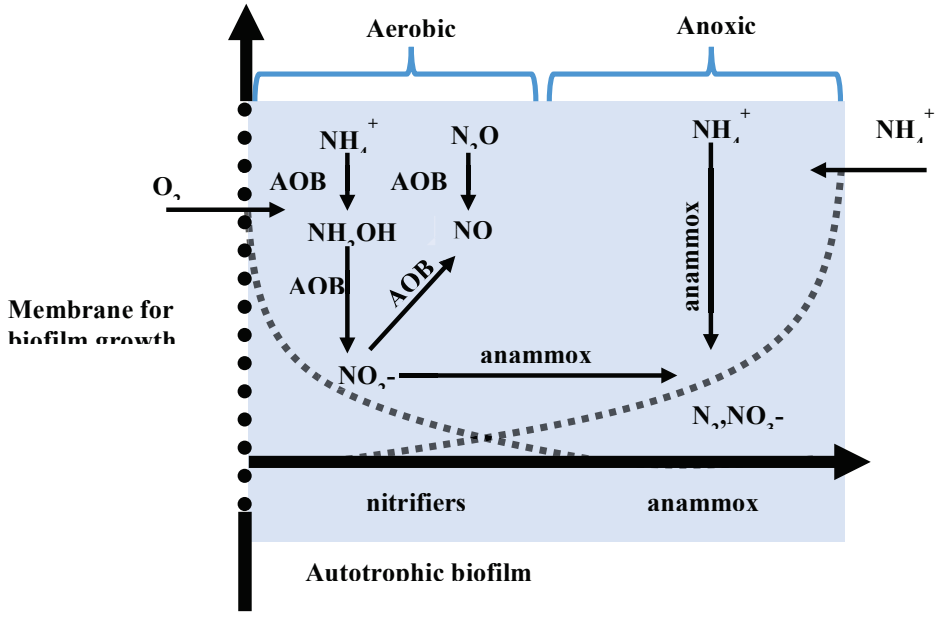

Figure 2. Microbial community structure and biological reactions including NO and N_2O production (drawn after *Baek et al.*, 2008)

2.1.4.2 The effect of operation conditions on microbial community structures and functions

Table 4 summarized the recent studies on microbial communities in MABR biofilms. The effect of process conditions on microbial community and the methods used to characterize microbial community were summarized in Table 4.

Table 4 The bacterial performance on different operation factors

Analysis method	Effect factors	Bacterial performance	Ref
Pyrosequencing the bacterial 16S rRNA genes	Influent pollutant concentration changing	Nitrifying bacteria growth accelerated	Tian et al., 2015
16S rDNA-based molecular technique Fish analysis	Gas flow rate Pressure	The Anammox active layer located in the region of anoxic liquid–biofilm interface, dominated by PLA46 and AMX820-positive Anammox microorganisms	Gong et al., 2008
DNA Extraction PCR Amplification DGGE Analysis	Oxygen concentration	An uneven spatial distribution of sulfate reducing bacteria. The maximum SRB biomass was located in the upper biofilm	Liu et al., 2014
The specific ammonium and nitrite oxygen utilization rate Fish analysis	COD/N ratio	With increasing substrate COD/N ratios, the specific oxygen utilization rates of nitrifying bacteria in biofilm were found to decrease, indicating that nitrifying population became less dominant	Liu et al., 2010
OTRs modeling	Oxygen transfer rates	Higher availability of ammonia at the biofilm base could be achived	Pellicer-Nàcher et al., 2013
Fish analysis	Oxygen Gradients	The cell density of ammonium oxidizing bacteria (AOB) was rela- tively uniform throughout the biofilm, but the density of nitrite oxidizing bacteria (NOB) decreased with decreasing biofilm DO.	Downing and Nerenberg, 2008
Pyrosequencing	Influent NH_4-N concentration	Anaerolineae, and Beta-and Alphaproteobacteria were the dominant groups in biofilms for COD and NH_4-N removal	Tian et al., 2016
Real-time quantitative polymerase chain reaction analyses	Sequential aeration	Population density changes, NOB nitrifying bacteria and nitrifying bacteria drastically reduced, AnAOB number increased by 10 times	Pellicer-Nàcher et al., 2014

Tian et al., (2015) found out that the microbial community strongly corresponded to the operational parameters. Bacteria in group V belonging to *Hirschia*, *Enterobacter*, *Proteocatella*, were negatively correlated with the influent NH_4-N concentrations. However, group X and XI bacteria, *Nakamurella*, *Micropruina*, and *Sediminibacterium*, showed positive correlation with the influent NH_4^+-N concentrations (Tian et al., 2015). Some of the groups had a positive correlation with influent COD and $NaHCO_3$ concentrations but showed a negative correlation with the inlet DO concentration. The NH_4^+-N and TN removal efficiency changed significantly

due to the shift of functional biomass but the COD removal ability showed a stable situation.

The heat map based on the OTU0.03 level can also explore the shift of microbial community with changes in operation process. The variation of flow velocity and influents led to a significant change of microbial community, which could be divided into eight groups (Ahmed et al., 2007). At a class level, *Gammaproteobacteria* and *Betaproteobacteria* had a positive correlation with influent COD and NH4-N. In contrast, *Deltaproteobacteria*, *Nitrospira, Chloracidobacteria*, and *VHS-B5-50* (candidate class) were negatively correlated with influent COD and NH_4-N (Tian et al., 2016). *Acidobacteria* and *Alphaproteobacteria* had a positive correlation with the flow velocity. The principal component 1 (PC1) and component 2 (PC2) occupied 73% of the variance in the microbial community. However, at the OTU level, PC1 and PC2 explained 34.6% and 31.4% variance of the bacteria in biofilms, respectively. The main reason for this phenomenon was that the change of the substrate transfer rate and physical characteristics in biofilm had a significant influence on bacteria community, which led the variable distributions of chemical and physical gradients and promotes biofilm formation (Tian et al., 2016).

Oxygen gradients have a significant effect on microbial community structure in MABR systems. Downing and Nerenberg (2008) found that the cell density of ammonium oxidized bacteria (AOB) was relatively uniform throughout the biofilm, but the density of nitrite oxidizing bacteria (NOB) decreased with a reduction in biofilm DO. There was no nitrate formation when the intra-membrane operating pressure was increased, where the NOB density was less than 10% of the AOB density. When the intra-membrane pressure reached at 70 kPa, the NOB population was constituted by 50% *Nitrobacter spp* and 50% *Nitrospira spp*. However, the concentration of *Nitrospira spp* would get around twice the concentration of *Nitrobacter spp* (Downing and

Nerenberg, 2008). Furthermore, no *Nitrobacter spp* could be detected at a distance greater than 30 μm from membrane at 14 kPa. Under the same operation conditions, the *Nitrospira spp* occupied the same density compared to the density at 35kPa. Very few NOB community could be detected at distance above 60 μm from the membrane surface (Terada et al., 2010). The O_2 concentration curve shows that O_2 permeates to the bottom of the breathable membrane and the O_2 is gradually consumed in the biofilm until it is completely depleted near the biofilm / bulk liquid interface, indicating the presence of oxic and anoxic zone in the MABR system (Pellicer-Nàcher et al., 2014). The H_2S concentration profile showed that H_2S production was found at 285 μm above the biofilm, indicating a high SRB activity in this region. The DGGE results of PCR amplification of isoimine reductase subunit B (dsrB) gene and FISH showed that the spatial distribution of sulfate reducing bacteria was not uniform. The maximum SRB biomass is located in the upper biofilm (Liu, et al., 2014). Pellicer Nàcher et al., (2014) based on FISH analysis of biofilm, pointed out the radial microbial stratification corresponded to the O_2 concentration. AOB bacteria community owns high cellular densities in the O_2 rich location where is close to the membrane surface, while the anaerobic ammonium oxidizing bacteria(AnAOB) microbial community located close to the bulk liquid, which is separated by a transition region supported by denitrifying HB bacteria.

The activity of nitrides in biofilms was inhibited by over-proliferation of heterotrophic organisms, which also explained why the performance was eventually deteriorated with experimental time (Liu et al., 2010). The biofilm activity test showed that the proportion of heterotrophic population over the nitrified population increased with an increase in the COD / N ratio of the substrate (Liu et al., 2010). Lin et al., (2016) tested the oxygen uptake rate of nitrifying and the heterotrophic bacteria under different C/N ratios. It was found that the carbon source was

important for a bacterial community development. If the carbon source was plentiful in a denitrifying process, the COD concentration barely affected the activity of nitrifying bacteria (Lin et al., 2016). Besides that, it was easy to achieve the balance between nitrification and denitrification. However, an insufficient carbon source in the denitrification process would break this balance and thus led to a low efficiency of MABR biological performance (Lin et al., 2016). The *Thauera sp.* density decreased with a decrease in the COD/N ratio (Lin et al., 2016). The density of *Sphaerotilusnatan* had the same trend with *Thauera sp*. At a COD/N ratio of 3, the biofilm became loose and the *Sphaerotilusnatan* disappeared completely (Lin et al., 2016).

2.2 Membrane performance of MABR

2.2.1 The impact of membrane module, materials and parameters

Different types of membrane modules and materials will result in different biological performance in MABRs. Table 5 summarized the membrane module parameters of MABR systems in recent studies.

Table 5(a) Membrane module parameters

Application	Membrane material	Working volume	Pore size	Working area	Thickness	Ref
COD removal	Polypropylene	190 ml	0.36 μm	4.048 m^2/m^3(specific surface area)	1.4mm	Ohandja and Stuckey, 2007.
	Polypropylene	2 L	/	/	30-40 μm	Xin et al., 2012
	Polypropylene	9.216 m^3	/	287 m^2/m^3	40-60 μm	Xin et al., 2012
	Coal	2.4 L	2μm	/	2.1 mm	Hu et al., 2008
	Coal	/	3 μm	0.18 m^2	2.1 mm	Liu et al., 2007
	Woven fabric silicon	2 L	/	0.26 m^2	/	Liao and Liss, 2007
	PVDF	9.5 L	3 μm	/	2.1 mm	Hu et al., 2009
	Polymer	/	/	10.28 m^2	70-90 μm	Li et al., 2016
	PVDF	/	/	/	150 μm	Tian et al., 2015
	PVDF	0.96 m^3	0.23 μm	235 m^2	/	Lai et al., 2015
	PVDF	9.5 L	2 μm	/	2.1mm	Hu et al.,2013
	Woven fabric Silicon	1.5 L	/	0.26 m^2	/	Zheng and Liao (2016)
	PDMS	16 ml	/	40 cm^2	50 µm	Lebrero et al., 2013
	PDMS/PVDF	8 ml	/	40 cm^2	/	Luvsanjamba et al., 2008
Air pollution control	Polypropylene	/	0.36 μm	4.048 m^2 m^{-3}	1.4 mm	Ohandja and Stuckey 2007
	PDMS/PAN	/	/	40 cm^2	PDMS 1.5 μm PAN 50 μm	Álvarez-Hornos et al., 2011

Table 5(b) Membrane module parameters

Application	Membrane material	Working volume	Pore size	Working area	Thickness	Ref
	/	/	/	40 cm^2	PDMS 1.5 μm PAN 50 μm	Álvarez-Hornos et al., 2012
	/	300ml	/	8300 cm^2	55 μm	Lebrero et al., 2014
	PVDF	26.1ml	0.1μm	2400 cm^2	/	Zhao et al., 2011
	nonporous silicone	2.5L	0.5 mm	25 m^2 /m^3	1.0mm	Li et al., 2016
	PVDF/HF	/	0.07 μm	2.08 cm^2	/	Nisola et al., 2013
	Polypropylene	2.6L	/	/	30-40 μm	Sun et al., 2015
	Coal	4L	0.1-0.3 μm	/	0.5 cm	Gong et al., 2007
Nutrient removal	Polypropylene	10L	0.1 μm	0.195 m^2	/	Ngo and Guo, 2009
	Polypropylene	2.41L	0.45 μm	0.34 m^2	/	Sun et al., 2009
	Coal	2.1L	10 μm	565 cm^2	/	Yu et al., 2011
	Polypropylene	8L	0.2 μm	0.1m^2	/	Dong et al., 2009
	Polypropylene	1.42L	/	84.5 m^2 /m^3	/	Li et al., 2008
	PVDF	3.8L	0.2 μm	0.453 m^2	0.7 mm	Lin et al., 2015

Nisola et al., (2013) investigated the difference of partial nitrification between microporous PVDF and composite PEBA 2533 coated PVDF. The lower levels of nitrate indicated that the HF coated with dense polymeric layer might promote the formation of AOB biofilm system. The main reason for different N removals was that the presence of PEBA as a coating layer provides an additional membrane resistance for O_2 transfer so that the O_2 permeation in the combination

HF will be lower than that in the uncoated PVDF. Compared with conventional MABR, the SBMABR will provide a more stable microbial community which means it could create the suitable survival environment for AOB and denitrifying bacteria (Sun et al., 2015).

Membrane materials can bring different physical characters of membrane to increase performance of MABRs. Liu et al., (2007) investigated the effect of membrane materials and found out that the profile of Ln(Cs-C) changed with time and the Ln (Cs-C) was in the range of 0.071 m/h for silicon membrane, as compared to that (0.18m/h) for carbon hollow fiber membrane. This result suggests that the carbon hollow fiber membrane provided better permeability and had better performance for oxygen transfer. Furthermore, the attached biofilm on the carbon hollow fiber membrane was 0.55 g TOC/m^2 which was the highest value, as compared to other materials. The great bacterial adhesive ability and high oxygen permeability indicated that carbon hollow fiber membrane was more suitable as a gas permeable carrier in MABR systems. The DOPA solutions modified the surface of PVDF hollow fiber membrane and thus enhanced the gas flux in MABR system. The gas permeation increased with an increase in the coating time or DOPA concentration (Hou et al., 2013). After the concaves are filled, the excess DOPA will block pores which result in increasing gas transfer resistance (Hou et al., 2013).

The change in the MABR configuration will also impact the performance of the MABR system. Casey, (2007) pointed out the liquid distributor in an MABR system would bring a viable and effective process. Liquid distributor design may have the most important impact on efforts to ensure a good flow distribution of the MABR reactor, but it is also important to consider that the realization of homogeneous mixing in the membrane module not only affects biomass asphyxia but also reduces the COD level to close saturation constant level. MABR combined with other

membrane biofilm reactors could enhance the system performance. Recently, the systems integration showed a new trend for public to improve membrane performance. The MABR was combined with a membrane coupled bioreactor to treat synthetic space mission wastewater (Chen et al., 2008). In phase III of the second Membrane-coupled Bioreactor (M2BR) experiment, the COD and total nitrogenous pollutant removal efficiencies both exceeded 90%. This confirmed that the MABR, which contains components that are fully compatible with microgravity conditions, could be used for long-term space missions to handle waste streams including urine, atmospheric condensate and used sanitized water (Chen et al., 2008). Wang et al., (2015) used an intermittently aerated membrane bioreactor with a mesh filter to remove COD, TN, and TP. Compared with other nutrients removal systems, the intermittently aerated membrane bioreactor displayed a higher removal efficiency for COD, TN, and TP (Wang et al., 2015). For nitrogen removal, the complete nitrification could be achieved in most cases, due to inserting the anoxic phase into the system, the denitrification was enhanced. For phosphorus removal process, polyphosphate accumulating organisms (PAOs) in a system could assimilate in aerobic phase, while denitrifying PAOs could contribute for both nitrogen and phosphorus removal in anoxic phase.

2.2.2 Membrane fouling and full-scale applications

2.2.2.1 Membrane fouling control

Membrane fouling is unavoidable in MABR systems. On the one hand, the growth of biofilm on membrane surfaces provides essential biomass for COD/BOD removal and nutrients removal. On the other hand, the formation of biofilm on membrane surfaces results in additional mass transfer resistance, particularly for the overgrowth of biofilm (thick biofilm layer). Thus, controlling biofilm thickness for optimal biological performance is essential for successful full-

scale applications of MABRs. Minimizing the membrane fouling can enhance the permeability and biological performance of the membrane. As compared to the activated sludge membrane separation reactor (AS-MBR), the biofilm membrane reactor, i. e. MABR, provides lower fouling rate than AS-MBR at the same aeration rate and flux loading rate (Phattaranawik and Leiknes, 2009).

Biological pollution is a relatively slow process, its role is the gradual decline in water flux, transmembrane and pressure gradually increased, mineral excretion gradually reduced. Controlling biological membrane fouling is a major challenge for MABR system. Treatment or prevention measures are not always effective. We need further research the advance technology to control membrane fouling. The Effect of operating parameters on membrane fouling may get attentions because by adjusting the membrane module and operating parameters can prevent biological fouling (such as adjusting configuration of spacers). Besides that, surface coating can prevent biofouling and it will be focused on the antifouling performance of the polymer brush layer formed by adsorption composite agglomerated core micelles.

2.2.2.2 Full-scale application of MABRs

Target correlations between the MABR and biological performance are complicated in the extensive variety of reactor design, membrane properties, operating conditions and waste water characteristics that exist. Despite this challenge, it is clear that the specific COD and nitrification rates obtained from the initial MABR tests are always higher than many other wastewater treatment techniques. While the challenges of MABR scale-up are still there, they seem to be three aspects that can be expected to be the largest application: total nitrogen removal, high rate treatment, and high strength COD removal (Syron and Casey, 2008).

An alternative design (The ZeeLung system) was developed for MABR to overcome some of the current technical and economic limitations preventing the full-scale application of this system (Stricker. et al 2009). The system used a new compact hollow fiber membrane, an unprecedented diameter. The two pilot units for the synthesis of high-strength industrial wastewater (4700 mg COD / L, 145 mg TKN / L) were successfully operated for 16 months. They are simultaneously subjected to COD removal, nitrification, and denitrification. Due to the high specific surface area (810 m^2 / m^3), the surface load rate can be kept at a low level (3.6 g COD / (m^2*d)) to maintain a thin biofilm and use low-pressure air (41 kPa) instead of high-pressure pure oxygen. Comparing high frequency and low shear intermittent air and liquid mixtures also effectively improve substrate transport but do not stabilize biofilm accumulation.

A comparative analysis of the cost of MABR and activated sludge provided the information of system advances (Casey et al., 2008). The membrane cost and cost of electricity were key parameters in determining the relative feasibility of conventional methods for membrane-based methods. The price of the membrane in the current market declined in recent years, while the energy costs raised steadily. Due to these reasons, the full-scale application of MABRs for waste water treatment may become a powerful driving force for further development.

The MABR systems have a potential for high rate treatment in full-scale application. Two cases were chosen for demonstrated purposes; Case 1 is a comparison between hollow fiber MABR system and conventional activated sludge process which both were designed for the treatment of 3780m^3/d municipal wastewater. Case 2 is another comparison between a pure oxygen MABR system and an existing high-purity oxygen activated-sludge system which were both used to treat 115200m^3/d waste water. Although full-scale data is still lacking in these two cases, it shows that the energy required for aeration and mixing of full-scale MABR system can be expected to

remove 3-4 times energy intensive of COD (0.25kWh/kg $COD_{removed}$) than CAS process (1.05 kWh/kg COD $_{removed}$). While the total energy cost of MABR is less than 40% of the comparable activated sludge process (Casey et al., 2008). A stable BOD removal efficiency of 99.4% could be achieved in membrane full-scale application while the COD removal efficiency was 93.8%. This system also could be used to reduce the concentration of SS due to membrane modules effectively separated ionic and solid species. The high SS removal efficiency could be kept at 99.3%. Besides these, the full scale system showed a potential to remove particulate and soluble phosphorus (Choi et al., 2017). Syron et al., (2015) successfully applied a 60L MABR to treat landfill leachate, which contains very high concentrations of insoluble chemical oxygen demand (COD) and ammonium. The air or pure oxygen is supplied to the bioreactor by a polydimethylsiloxane hollow fiber membrane. After one year of operation, the average hydraulic retention time of about 5 days, the influent concentration range of 500 ~ 2500 mg / L, MABR nitrification to 80-99%. At the same time, the ranging from 1000 to 3000 mg / L of influent COD concentration decreased by about 200-500 mg / L.

In the closed-loop life cycle support system, the bioactive membrane aeration MABR can reduce the dissolved organic carbon and ammonia concentrations and reduce the pH of the wastewater, resulting in a more stable solution Less potential to support biological growth or to promote the delivery of non-ionized ammonia and to produce higher quality brine. Sevanthi et al., (2014) developed the CoMANDR 2.0 system to assess the effect of specific surface area (200 m^2 / m^3) and to investigate the effects of low total air flow and forced hibernation (no dwelling time) in the system. The system supplied unstable wastewater from donated urine, ersatz sanitation, humidity condensate and laundry water every day. Continuous monitoring of liquid side system pH, TDS, DO and temperature, daily monitoring of DOC, TN, NOx and NH_4 water and effluent.

The gas side system continuously monitors O_2, CO_2, N_2O intermittently monitored in the exhaust gas. The results supported the ability of the system to effectively reduce organic carbon by more than 90% and convert 70% of the total influent N into a non-organic form such as NOx or N_2. ZeeLung's ability to improve total suspended solids and ammonia removal, which are both benefits of the system's ability to increase biomass inventory without increasing mixed liquor suspended solids concentration. With the potential to reduce energy demand as well as intensify nutrient removal, ZeeLung MABR can help wastewater treatment facilities move from significant energy users toward becoming energy neutral facilities. ZeeLung MABR offers an innovative way for us to meet future regulations for nutrient removal within the plant's existing footprint.

2.3 Modeling learning

Due to many operation factors would impact the MABR systems, many researchers established a mathematical model to figure out the situation of biofilm (Casey et al., 1999). So the first wave of the concepts of modeling for MABR is to describe the phenomenon of biofilm inside. However, after this kind model used to application. The authors (Casey et al., 1999) found the model for suspended biomass is inadequate. They try to remedy this problem by including reaction-diffusion mass balances. The following is reaction-diffusion model. A steady-state approach ($dC_s/dt=0$) based on Fick's law was used.

$$D_S \frac{\partial^2 C_S}{\partial Z^2} = r_s \qquad (3)$$

$$r_s = \mu_{max} * \frac{1}{Y_{X/S}} \frac{C_S}{C_S + K_S} X \qquad (4)$$

Where D_S is the substrate diffusivity, m^2/s, C_S is the substrate concentration, g/m^3, r_s is the substrate conversion rate, μ_{max} is the bacteria maximum growth rate,1/s, K_S is the substrate half-saturation constant, g/m^3, $Y_{X/S}$ is the biomass yield based on substrate, X is the biomass density, g/m^3

In order to expand the full-scale application of MABR systems, more and more researchers focused on mathematic modeling to simulate the MABR performance (Casey et al., 1999). Thus, the optimal operating and environmental conditions and the microbial community functions can be identified. Table 6 summarized some recent studies on mathematic modeling.

Table 6 Membrane modeling and assumptions

Model equation	Assumptions	Ref
$\frac{\partial C_{O2,g}}{\partial t} = \frac{\partial}{\partial x}\left(D_g \frac{\partial C_{O2,g}}{\partial x} - u_g C_{O2}\right) - \frac{2}{R_m} K_m (C_{O2} H_{O2} - C_{O2,l})$ for O_2 $\frac{\partial C_{N2,g}}{\partial t} = \frac{\partial}{\partial x}\left(D_g \frac{\partial C_{N2,g}}{\partial x} - u_g C_{N2}\right) - \frac{2}{R_m} K_m (C_{N2} H_{N2} - C_{N2,l})$ for N_2	the membrane had the same Km value for O_2 and N_2	Perez-Calleja et al., 2017
$OUR(z) = \mu_{MAX,AOB} - (\frac{3.43 - Y_{AOB}}{Y_{AOB}}) \frac{S_{NH4}(z)}{S_{NH4}(z) + K_{NH4}} \frac{S_{O2}(z)}{S_{O2}(z) + K_{O2}} X$	mass transport in the boundary layer is diffusion-limited $k_L = \frac{D_{O2}}{L_{BL}}$ the overall mass transfer coefficient to also depend on an additional biofilm mass transfer coefficient (kB, m/d) that varies with biofilm activity	Pellicer-Nàcher et al., 2013
$D_{OB} \frac{d^2 O}{D_{y^2}} = \frac{X_{\mu_m}}{Y_{X/S}} \frac{O}{K_O + O} \frac{S}{K_S + S}$ $D_{SB} \frac{d^2 S}{D_{y^2}} = \frac{X_{\mu_m}}{Y_{X/S}} \frac{S}{K_S + S} \frac{O}{K_O + O} + r_{S,ZERO}$	1.There is no diffusional resistance in the gas side of the membrane. 2.The biofilm is assumed homogeneous and the thickness is uniform along the length of the membrane. 3.The bulk liquid is well mixed and there are no axial gradients along the surface of the biofilm.	Syron and Casey, 2008
OTR=nUA(m$C_{int} - y_0$) $*$ [exp $\left(-\frac{\pi d \ K_g}{UA\delta} * Z\right) - 1$]	the DO concentration used in the model is assumed to be at the interface between the membrane and the liquid C_{int} . C_{int} in the expression for flux above was assumed not to vary with distance along the fibers and, hence, to be a user-defined constant.	Gilmore et al., 2009
$\frac{\partial C}{\partial t} = \frac{-v_x \partial C}{\partial z} + \varepsilon_x \frac{\delta^2 C}{\delta x^2} \pm k_o a\ (D_{o_2}) \pm r_{BIO}$	Nutrient transport and biochemical condition are independent processes	McLamore et al.,2007
$\frac{\partial S}{\partial t} = D_{eff,S} \frac{\partial^2 S}{\partial y^2} - (\frac{X\mu}{Y_{X/S}})$ for phenol $\frac{\partial S}{\partial t} = D_{eff,S} \frac{\partial^2 S}{\partial y^2} - (\frac{X\mu}{Y_{X/S}})$ for oxygen	There are no axial gradients in substrate concentration in the membrane module and the biofilm thickness is uniform. The biofilm is homogeneous, and that the mass transfer through the mass boundary layer and within the biofilm is diffusional and per- pendicular to the biofilm surface.	Syron,et al., 2009
$L_{O2} = K_{O2}(\frac{S_{O2,g}}{H_{O2}} - S_{O2})$ $J_{O2} = \varepsilon D_{O2} \frac{\partial S_{O2}}{\partial Z}$	The chemical oxidation of sulfide was not included in the model. The rates of the growth of microorganisms were modelled using Monod-type kinetics while the microorganism decay was simulated through first-order kinetics as suggested in the Activate Sludge Model No.1	Sun et al., 2017
$J_{O2} = Ak_i(\frac{C_{O2,g}}{m} - C_{O2})$	$v_d = u_f(\frac{L_F}{L_{F\,max}})^{10}$	Matsumoto. et al., 2007
$J_{O2} = nQ_{air}(HS_{O2,F} - S_{O2,G})[\exp\left(-\frac{\pi d D_{O2,silicone} K_G l}{Q_{air}\delta}\right) - 1]$	$A = \pi nl(d + 2\delta + 2Z)$ $u_{de} = u_F(\frac{L_F}{L_{F\,max}})^2$	Landes et al., 2013
$r_N = k_N Xf \frac{S}{S + gk_N} \frac{DO}{DO + k_O}$ $f = \frac{1}{1+10^{(6.5-pH)}}$ $g = \frac{1+10^{(8.5-pH)}}{1+10^{(6.5-pH)}}$	Acidebase reactions are instantaneous The partial pressure of carbon dioxide remained constant at 0.0004 atm on the gas side of the membrane	Shanahan and Semmens,2015

2.3.1 Mass transfer modeling research

Mass transfer at the membrane-biofilm and biofilm-bulk wastewater interfaces is critical for the

supply of oxygen and substrates to active biofilm layer for biodegradation. And mass transfer at the interfaces is a result of the flow conditions in the bulk phase and can be calculated if the empirical derivative relationship between the flow and mass transfer is available. Many researchers investigated the factors effecting mass transfer such as operation and environmental conditions, configurations.

MABR systems can be operated as open-ended or closed hollow fiber membranes. However, the system with closed HFMs suffered from gas back-diffusion which would cause membrane low performance. On the other hand, there is a large amount of gas lost in the open-ended process. Although the high gas velocity can achieve greater mass transport, it leads greater energy consuming. One method is periodically opening the membranes to vent back-diffusion gases. Due to this advantage, studies were conducted to explore periodic venting of hollow-fiber membranes as a mean to maximize the oxygen transfer efficiency (OTE) and oxygen transfer rates (OTR) of MABRs. Different venting intervals ranging from 1 to 30 mins were simulated in this modeling research, with a constant venting duration of the 20s (Perez-Calleja et al., 2017). The predicted average OTRs were 2-4 times higher than a system with the permanently closed end and OTE values were significantly higher than that of the open end systems. OTR can be higher than continuous open operation when the venting interval is short enough (Perez-Calleja et al., 2017). This new gas supply strategy can significantly improve the ability of MABR to reduce the capital and operating costs of the new system. Pellicer-Nàcher et al., (2013) found the factors affecting oxygen mass transfer across membranes during clean water tests and reactor operation by un-disturbing microelectrode inspection and bulk measurements. The results suggested that the nitrifying biofilms in MABR system fully utilized oxygen when operation conditions are under simultaneous NH_4 excess (the concentration 50 times K_{NH4AOB}) and oxygen

limitation. This condition significantly enhanced the rate of oxygen uptake in the deeper biofilm region. From a design point of view, the biological reactor configuration, in which each stage has an installed membrane area, used to reduce the ammonium removal rate and to optimize oxygen consumption appears to be ideal. The mass transfer resistance of the liquid boundary layer developed at the membrane–liquid interface during clean water tests took account of two-thirds of the total mass transfer resistance, suggesting a strong underestimation of the oxygen transfer rates when it was absent.

An oxygen transfer model was applied to simulate the performance of a hollow fiber membrane biofilm reactor (Casey 2007). The proposed mathematical model was a reasonable prediction of OTR in HFMBR with active biofilm. The OTR with the active nitrifying biofilm was significantly higher than the OTR predicted by a large amount of liquid clean water test (Casey 2007). The measured mass transfer coefficient showed a slight positive correlation with the fiber lumen pressure. When the biofilm existed on the membrane surface, the material based material model represented the oxygen transfer conditions, but it required measurement or assuming the actual membrane-biofilm interface DO concentration. However, the model maintained simplicity of solving and utility in the design of redox-stratified biofilms these advantages compared with other OTR predictors (Gilmore et al., 2009). The transport abiotic model allowed MABR transport to be characterized by biotransformation efficiency in this nitrification case. MABR had been proved to be suitable for a wide variety of waste water treatment. This model would help maximize transport while transforming target pollutants at the same time. The results of mass transfer and hydrodynamic analysis show that MABR can be modeled with a Christian Michelsen Research regime where axial dispersion is moderately low. The model data

showed that oxygen mass transfer and nutrient convection might limit biofilm reactor performance (McLamore et al., 2007).

The efficient oxygen utilization is a key point in MABRs system simulation. Syron and Casey (2008) investigated the potential of MABR system for high-rate bio-oxidation. A preliminary hollow fiber MABR process combined with a reaction-diffusion model was used to research reaction rate-limiting mechanism and to perform comparative analysis on prospective designs and operational parameters. When the intra-membrane oxygen pressure is high enough, the high oxidation fluxed will be achieved in the MABR. But the volumetric oxidation rate was depended on the specific surface area of the membrane which meant the maximum performance was achieved in MABRs with thin fibers. This result showed when the COD concentration was not particularly high, an advantage would not be attained by designing the thickness of membrane even if the oxygen limitations can be solved. Since the volume removal rate was largely dependent on the membrane specific surface area, the MABR design with thinner films appeared to be superior to high volumetric oxidation rates. Syron et al., (2009) developed a simple mathematical model to study the utilization of self-suppressing matrices in idealized biofilm reactors using counter diffusion or co-diffusion of oxygen and phenol. The unsteady state of the model was used to study the effect of the impact load of phenol on the biofilm performance. It proved that the counter diffusion configuration might be advantageous at high phenol concentrations if the biofilm thickness was above the critical value. The performance advantage of the counter diffusion configuration was obtained by the presence of an oxygen depletion layer adjacent to the liquid biofilm interface, which served as a diffusion barrier for phenol transport to the respiratory activity area.

2.3.2 MABR performance modeling research

Combining mathematic model with MABR systems, researchers can predict the membrane and biological performance and easier to find the optimal removal efficiency. A mathematical model was used to evaluate the sulfide oxidation and sulfur production of MABR in the presence of residual organics in the influent. It was calibrated and validated using the experimental data from the long-term operation of the sulfide-oxidation MABR at different operational stages. Sulfide loading and oxygen pressure could be combined to find an optimal zone to achieve a high sulfur recovery efficiency (>75%). While the biofilm area to reactor volume (A/V) ratio could influence the sulfur recovery efficiency. When the oxygen pressure was 60kPa and influent sulfide concentration was 500 mg S/L in this modeling research, the optimal A/V ratio should be $150m^{-1}$ (Sun et al., 2017). Vafajoo and Pazoki (2013) evaluated operating parameters to predict nutrients removal efficiency on completely autotrophic nitrogen removal over nitrite (CANON) process which is a combination of partial nitrification. In this study, modeling of anaerobic ammonia oxidation (ANAMMOX) process and partial nitrification process were combined and a MABR system performed under constant volume and operation conditions. The modeling of CANON process was demonstrated through the Active Sludge Model 3 (ASM3) reference model. It was displayed that, when the ammonium concentration was 130 g N/m^3 and DO was 1.3g O^2/m^3, the optimal nitrogen removal could be achieved with 0.7 mm biofilm thickness.

A multi-population biofilm model for fully autotrophic nitrogen removal was developed and implemented in the AQASIM software to research the stratification and total nitrogen removal characteristics in the membrane aerated biofilm reactor (Zhao et al., 2010). According to calculation results, the flux ratio of oxygen and ammonia (J_{O2}/J_{NH4}) was an important factor

which could affect the population stratification. If the value of J_{O2}/J_{NH4} was less 0.25, no stratification appears. With J_{O2}/J_{NH4} increased, the time of stratification onset decreased quickly. When the value reached to 1.5, stratification time would get the shortest time. When J_{O2}/J_{NH4} exceeded 1.5, the stratification time increased successfully. Once the biofilm reached a certain thickness, the anaerobic ammonium oxidant could grow and form an anaerobic zone. When J_{O2}/J_{NH4} remained constant at 1.5, the total nitrogen removal efficiency increased with the increase in biofilm thickness. However, if the thickness of the biofilm exceeded 2.0mm, the total nitrogen removal efficiency will drop immediately, which may be due to the difficulty of diffusion in the thicker biofilm.

A mathematical model was used to evaluate the NO and N_2O production potentials in membrane aerated autotrophic biofilms under various operating conditions. The AOB-mediated denitrification pathway was used to simulate NO and N_2O production. According to results, the yield coefficient and maximum biomass specific reaction rate of AOB directly affect N_2O production rates. Reducing NO and N_2O production by controlling the oxygen surface loading rate may affect N removal performance. It still had a conflict between optimal nitrogen removal (75%) and minimum NO and N_2O production (TN removal rate of 0.5%) during ammonium surface loading changes. Based on the correct model structure, a relatively low NO and N_2O production (less 1.0%) could be achieved in MABR by controlling the oxygen and ammonium surface loading to promote anammox growth. Steady-state biofilm thickness had a significant but different effect on TN removal and NO and N_2O production. When the biofilm thickness was less than 1000 mm, an increase in the steady-state biofilm thickness results in an increased TN removal and a decrease in NO and N_2O production. However, when the biofilm thickness was greater than 1000 mm, it had opposite effect. From this, it indicated an optimum thickness of

about 1000 mm (Ni and Yuan 2013). Another multi species one-dimensional biofilm model considered nitric oxide and nitrous oxide productions for MABR system. This model was used to evaluate how periodic aeration as a control parameter reduced NO and N_2O production when the system kept a high TN removal efficiency. Factors that control the Anammox activity in MABR indicated that enhanced Anammox activity not only contributed to high levels of nitrogen removal but also reduced NO and N_2O production. Aeration strategy (periodic aeration versus continuous aeration) showed that periodic aeration could reduce NO and N_2O production by promoting Anammox growth to maintain high nitrogen levels (Ni et al., 2013).

2.3.3 Microbial community structure modeling research

It is important to evaluate the microbial community compositions inside bioreactors used for waste water treatment because it will determine the microbial composition in the effluent and impact waste water treatment requirements for pollutant removal efficiency. Matsumoto et al., (2007) used the simulation software AQUASIM 2.1 to develop a multi-model modal of membrane-permeable biofilm considering HB, AOB and NOB. This model confirmed that the high-oxygen (COD) and nitrogen removal efficiency. Besides this, it accurately predicted COD, NH_4^+-N, and T-N removal efficiency, and determined the COD/nitrogen (C / N) ratio, biofilm thickness and oxygen surface load, which could significantly affect the simultaneous nitrification and denitrification efficiency. A high denitrification efficiency (greater than 70%) was achieved in the C / N ratio range of 3.0 to 5.25 and the biofilm thickness range of 600 to 1200 μm.

Now the tracer experiment and Residence Time Distribution (RTD) theory will characterize the flow in a particular MABR system. The liquid phase flow pattern was researched by using tracer pulsed stimulation where dextran blue was as a tracer. According to the experimental results of RTD simulation, it was proved that the flow pattern was similar to the completely mixed flow,

which had the ideal hydraulic dynamic behavior deviation. The high ammonia oxidation under AOA-driven oxygen-limited conditions compared to ammonia-oxidizing bacteria (AOB) may be more suitable for autotrophic nitrogen in a single-membrane membrane biofilm reactor coupled to anaerobic ammonia removal of oxidation (Anammox) (Plascencia-Jatomea et al., 2015).

There is a strong relationship between the characteristics of nitrifying bacteria community and DO concentration. Based on the research results, it showed that the stable nitrification efficiency of the optimal DO concentration was higher than 5.0 mg/L. As a result of DGGE and cloning, the proportion of AOB community and Nitrosomonas changed minimally even the nitrification efficiency is different. Besides that, higher DO concentrations caused an increase in AOB and NOB, but it also led a reduction in heterotrophic microbes. INT-dehydrogenase activity (DHA) test showed that with the decrease of DO concentration, the activity of AOB decreased. This indicated that the DO concentration did not affect the AOB community, but affected the AOB activity. In the relationship between the biomass and the nitrification efficiency, only the activated biomass affected the nitrification efficiency (Park et al., 2008).

2.3.4 The effect of operation conditions on modeling research

Evaluating the effect of operating conditions is important for researchers who can find the best situation to control the MABR system increasing the removal performance. The alkalinity and pH value affection on nitrification in a MABR system can be evaluated by a one-dimensional biofilm model. The concentration distribution of dissolved oxygen, ammonium, nitrate and pH in the biofilm and the overlying boundary layer was measured by a shielded microelectrode under actual operating conditions. Nitrification in the membrane-aerated biofilm was shown to substantially reduce local pH close to the membrane support. The pH drop depended on the influent alkalinity/ammonium concentration ratio. The Hydrocarbon alkalinity provided a good

pH buffer in the pH range of 5-7, and if there was insufficient bicarbonate, the pH might drop to more acid values. The bicarbonate alkalinity of the influent strongly affected the nitrification properties of MABR, even if the reactor is equipped with a pH controller that provided NaOH to keep the pH close to 7.5. When the influent carbonate concentration increased from 0.6 to 4.8 mM, the nitrification of MABR also increased from 65% to 77% (Shanahan and Semmens, 2015).

The no-invasive micro sensor techniques can investigate the real time changing in oxygen and proton fluxes of mature *Nitrosomonas europaea* and *Pseudomonas aeruginosa* biofilms in MABR system under exposing to environmental toxins. And characterized stress response during exposure to toxins with known mode of action (chlorocarbonyl cyanide phenyl-hydrazone and potassium cyanide), and four environmental toxins (rotenone, 2,4-dinitrophenol, cadmium chloride, and pentachlorophenol). The result showed that rotenone (25-50μM) would cause a temporary increase in O_2 influx, however, it did not significantly affect H^+ flux; when the concentration of $CdCl_2$ was 5 μM, the O_2/H^+ flux for both species would increase; PCP caused the largest peak increase in O_2 flux relative to all other toxins (Mclamore et al., 2010). In addition, the characterization of bulk liquid-biofilm physiological H^+/O_2 transport will improve our understanding of data collected from real time bulk liquid monitoring, and will aid in the development of dynamic simulation models (Mclamore et al., 2010).

2.4 Thermophilic aerated biological treatment

The thermophilic aerated biological treatment (TABT) is one of the well-recognized technologies for the treatment of sludge produced by municipal wastewater treatment plants. In this type of bioreactor, the temperature rises over 50℃ due to the conservation of a part of the

heat produced by the aerobic metabolism of the microorganisms that consume the abundant organic material present in the sludge (Juteau. 2006). It already became popular used in wastewater plants because it provided us rapid biodegradation rate, low sludge yields and excellent process stability (Collivignarelli et al., 2015). Since the first step of its development, aerobic thermophilic digestion has been proposed as a method for treating livestock waste in liquid form. This applies mainly to pig manure, but in some cases also to cow dung. In addition to the effect of killing pathogens, the claimed advantages are also the simplicity of the method, its robustness, higher reaction rates and therefore smaller bioreactors), the possibility of nitrogen storage and heat recovery (Juteau, 2006). However, this treatment system still faces some problem such like poor flocculent potential and foaming bacteria problems.

3. Research objects

The overall goal of this study is to develop next generation of technologies for sustainable wastewater treatment. More specifically, this study will focus on the theoretical and modeling analysis of a novel type of ThMABR technology for wastewater treatment. Specific objectives are:

1. To prove temperature has positive effects on MABR based on combination reactors
2. Characterize the diffusion-reaction process based on modeling
3. Make a comparison about membrane performance between thermophilic MABR and mesophilic MABR based on simulation results
4. To prove the modeling is reasonable based on case study

3.1 Novelty points

A modeling research focus on temperature factors effects between thermophilic and mesophilic MABR system has not been reported.

4. Research method

4.1 Theoretical Analysis of the Impact of Temperature on Biofilm, Water and Mass Transfer Characteristics

As a biological treatment system, the ThMABR is mainly composed of membranes for oxygen delivery, and biofilms formed on membrane surfaces for biodegradation. Oxygen, pollutants and nutrients are transferred into the biofilm for biodegradation in a counter-diffusion manner. Among various factors that affect the performance of MABR, temperature plays a dominant role. A change in temperature results in changes in biofilm characteristics (thickness, density, porosity, growth and detachment rates, microbial community, biodegradation rate etc.), water and gas properties (viscosity, surface tension, density etc.), membrane properties (pore size, tortuosity, solubility) and transport properties (diffusivity, flux, permeability). In return, these properties have a profound effect on the overall performance of ThMABR.

4.1.1 Impact on Biofilm Properties

As shown in Figure 3, biofilm is the layer between the membrane surface and the bulk water phase, and mainly consists of microorganisms, extracellular polymeric substances (EPS) -which are excreted by the cells and which immobilize these cells and entrap particles within the matrix of biofilm. Biofilm is one of the most important components in MABR, as physical, chemical

and biological properties of biofilms determine diffusion and biodegradation rates within biofilm. Although extensive studies have been conducted on biofilms, literature review indicates that most temperature-related studies focus on the formation of biofilm and very little attention has been paid to the impact of temperature on physical and chemical properties such as oxygen transfer rate and membrane performance. Zhang and Bishop (1994) found that the freezing technique in preparing biofilm samples for micro-slicing had no obvious adverse effects on biofilm properties (density, pore size etc.) as compared to that of the control samples. Overall, there is a lack of fundamental information on the temperature impact. However, it is clear that when the temperature is changed from the mesophilic (25-35°C) to the thermophilic (45-65°C) range, different microbial communities will be expected (LaPara et al., 2000) Thermophiles will survive at thermophilic temperatures and mesophiles will grow at mesophilic temperatures.

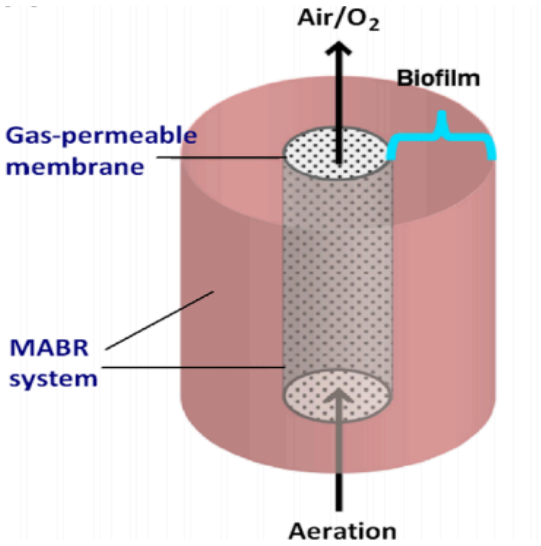

Figure 3. Schematics Diagram of Membrane Aerated Biofilm Reactor(MABR)

It is generally assumed that substrate consumption rate r_c within biofilm can be described by Monod equation with oxygen and organic substrate (C_s and C_o):

$$r_c = \mu_{max}\left[{}^{C_s}/_{(K_s + C_s)}\right]\left[{}^{C_o}/_{(K_o + C_o)}\right] \quad (5)$$

Where K_s is the substrate half-saturation constant, K_o is the oxygen half-saturation constant

In general, biodegradation rates are doubled for every 10 ^{o}C increase, in the range of 5-30 ^{o}C. A comparison of the biodegradation rate between the mesophilic and the thermophilic temperature may be difficult, owing to changes in microbial communities. However, it is generally accepted that biodegradation rates in thermophilic temperatures are much higher (3-10 times) than these in the mesophilic temperature range. Lapara and Alleman (1999) summarized the available biokinetic constants for the temperature range from 20 to 58 °C. According to these figures of biokinetic constants against temperature, the maximum specific rate of microbial growth, maximum specific rate of substrate utilization and endogenous decay rate are a strong function of temperature. Although these data are obtained from the suspended growth biomass, it is believed, in principle, that similar trends will be observed for attached growth biomass.

Diffusion in biofilms is a complicated process, due to the heterogeneity nature of biofilm structure. Pore size of channels, porosity, tortuosity and thickness of biofilm affect the diffusivity of oxygen and substrate. Some researchers assume the diffusivity in biofilms is equal to that in water, considering the majority of biofilm is water (Reij et al., 1998), while others consider the diffusivity in biofilm as an effective diffusivity, which is equal to the diffusivity in water times the physical parameters of biofilm (porosity, tortuosity, pore size) (Rincon et al., 2013). López et al., (2003) explained following equation to estimate the effective diffusivity in biofilms.

$$D_{eff} = (\varepsilon D_W)/\tau \quad (6)$$

Where ε is the porosity of biofilms, τ is the tortuosity factor, D_W is diffusivity of water, m^2/s.

A change in temperature affects not only physical properties of bulk solution but also physical properties of biofilms. As a result, the effective diffusivity in biofilms increases with an increase in temperature.

The impact of temperature on biofilm growth rates is generally well understood. However, very limited information is available in terms of the influence of temperature on detachment rates. It is generally believed that thermophilies have a poorer flocculating ability than the mesophiles, e.g. the thermophilies have a dispersing growth nature. In addition, more substrate is converted to carbon dioxide and water instead of cell mass at thermophilic temperatures. Consequently, it is reasonable to believe that the growth rate of thermophilic biofilm thickness will be lower than that of the mesophilic biofilms under similar testing conditions.

4.1.2 Impact on Water and Gas Properties

It is well known that physical properties of water and gas are strong functions of temperature (Al-Shemmeri et al., 2012). Empirical equations are as follows to correlate physical properties of water and gas with temperature:

Viscosity of water equation accurate to within 2.5% from 0 °C to 370 °C (Al-Shemmeri et al., 2012):

$$\mu(w) = 2.414\times10^{-5}\times10^{2.478/(T-140)} \quad (7)$$

where T has units of Kelvin, and $\mu(w)$ is the water viscosity which has units of N*s/m^2.

Sutherland's formula can be used to derive the dynamic viscosity of an ideal gas as a function of the temperature (Smits et al., 2006):

$$\mu(g) = \mu_0(T_0 + C)(\ /T_0)^{1.5}/(\ T + C) \quad (8)$$

Where $\mu(g)$ is dynamic viscosity of gas (Pa·s or μPa·s) at input temperature T, μ_0 is reference viscosity (in the same units as μ) at reference temperature T_0, T is input temperature (K), T_0 is reference temperature (K), C is Sutherland's constant for the gaseous material in question.

Lapara and Alleman (1999) provides an excellent summary on physical properties of water at thermophilic temperatures. It is concluded that an increase in temperature from the mesophilic to the thermophilic temperature range reduces the viscosity and surface tension of water and increase mixing and colloids solubility in water, which will improve oxygen, pollutants and nutrient transfer rates. In addition, the increase in temperature reduces the saturation oxygen concentration in water and thus increase oxygen driving force across the membrane and enhances oxygen transfer.

In bulk liquid solution, diffusivities of oxygen and substrates are proportional to T / μ That is

$$\frac{W_T}{W_{T2}} = \frac{T}{T_2}\frac{\mu T}{\mu T_2} \qquad (9)$$

where D_W is the diffusion coefficient in water, m^2/s, T_1 and T_2 are the corresponding absolute temperatures, μ is the dynamic viscosity of the solvent. An increase in temperature results in a decrease in bulk liquid solution viscosity. Accordingly, diffusivities of oxygen and substrates in biofilms is proportional to T^n (n >1) (e.g. an increase in temperature leads to an increase in diffusivities in bulk liquid solution). The diffusivity of oxygen in the bulk liquid solution is increased from 2.1 $x10^{-5}$ cm^2/s at 25°C to 4.67 $x10^{-5}$ cm^2/s at 60°C (Essila. 1998).

In the lumen side of membranes, oxygen transfer to the biofilm involves adsorption, diffusion and desorption processes. An increase in temperature will slightly increase gas viscosity but reduce gas density. According to the Chapman-Enskog kinetic theory, diffusivity of oxygen in the bulk gas solution is proportional to $T^{1.5}/\mu$ That is

$$\frac{AB(T\ )}{AB(T2)} = \frac{T}{T_2}^{1.5} \left(\frac{\mu T}{\mu T_2}\right) \quad (10)$$

An increase in temperature results in a decrease in viscosity. Consequently, diffusivity of oxygen in the bulk gas phase is proportional to T^m (m>1.5). Estimation indicates that the diffusivity of oxygen in air is increased from 0.203 cm^2/s to 0.264 cm^2/s when the temperature is increased from 20℃ to 60℃ (Richard. 2005).

4.1.3 Impact on membrane properties

Temperature has a significant impact on polymeric membrane properties. An increase in temperature results in an increase in pore size, due to the impact of swelling (Simon et al, 2013), thus a high flux or permeability will be anticipated at a higher temperature. In addition, an increase in temperature leads to a lower solubility and higher diffusivity of oxygen in membranes. Empirical correlations based on previous research data (Li et al., 1994) are regressed using Arrhenius Equation as follows:

Oxygen solubility in Polydimethylsiloxane (PDMS) membrane:

$$S_{O_g} = 3.88014\times10^{-11}\times e^{-58322.13/RT} \quad (11)$$

(Gas - PDMS membrane interface, T= 293-313K)

$$S_O = S_{O_g}\times H \quad (12)$$

(Water - PDMS membrane interface, H-Henry's constant is 0.0635, T=273-333K)

Oxygen permeability in PDMS membrane:

$$_{O_g} = 1.1042\times10^{-11}\times e^{-47\ 01/RT} \quad (13)$$

(Gas-PDMS-Gas, T=293-313K)

Effective diffusivity of oxygen in membrane is a function of pore diffusivity, porosity of membrane, and the solubility of oxygen in membrane and is expressed as follows:

$$D_{eff} = \frac{\text{AB}\varepsilon}{\varepsilon+(1-\varepsilon)\ \text{Og}} \qquad (14)$$

Temperature is an important factor which has significant degradative effects on membrane filtration, because the nature of seasonal changes in the temperature of raw water.

4.2 MATHEMATICAL MODELING OF THE IMPACT OF TEMPERATURE ON THE PERFORMANCE OF TMABR

Based on theoretical analyses and the fundamental equations that correlate the temperature and parameters mentioned above, a counter-diffusion and reaction mathematical model was developed, with the temperature impact incorporated, to study the transport and reaction processes in ThMABRs. Of particular interest is the comparison of the performance between MMABR and ThMABR. This model is characterized one hollow fiber biofilm membrane and assumption is operation conditions are equal for another hollow fiber module.

The following set of equations was developed and used for cylindrical hollow fiber membranes by arthor and assumed the flux into each membrane is equal. Oxygen flux to bulk water solution without biofilms on membrane surface can be described like following (Ntwampe et al., 2008):

$$\text{J} = \left(\frac{P_m * H}{L}\right)\left(\frac{32 * P_O}{H} - C_O|r = r_{\ f-in}\right) \qquad (15)$$

where $_m$ is the permeability of oxygen, gmole*m/(m^2*s*atm); H is Henry's constant of oxygen, atm*m^3/mole; L_e is the effective thickness of silicone membrane, m; $_O$ is the partial pressure of oxygen, atm.

Under steady-state conditions, based on Fick's law and Monod kinetic equation, the diffusion and reaction of oxygen and substrate within biofilms can be described using the following equations (Cao et al., 2009 and Tanase et al., 2011):

$$D_{Oeff}\left[\frac{d^2C_O}{d\ _2}+(\frac{1}{r})\frac{dC_O}{dr}\right]-\left[\frac{\mu_m S}{K_S+S}\right]\left[\frac{C_O}{K_O+C_O}\right]\frac{X_{bf}}{Y_{XO}}=0 \quad (16)$$

$$D_{Seff}\left[\frac{d^2S}{d\ _2}+(\frac{1}{r})\frac{dS}{dr}\right]-\left[\frac{\mu_m S}{K_S+S}\right]\left[\frac{C_O}{K_O+C_O}\right]\frac{X_{bf}}{Y_{XS}}=0 \quad (17)$$

where D_{Seff} and D_{Oeff} are the effective diffusivity of substrate and oxygen in biofilm at temperature T, respectively, m^2/s; K_S and K_O are the half-saturation constant of substrate and oxygen at temperature T, respectively, g/m^3; μ_m is the maximum specific growth rate at temperature T,1/s; Y_{XS} and Y_{XO} are the biofilm yield based on substrate utilization, oxygen consumption for biofilm growth and decay, respectively; $X_{\ f}$ is the density of biofilm, g/m^3.

Then based on mass balance, the flux comes into membrane equals the flux comes out from biofilm. The boundary conditions are following (Jiang et al., 2018 and Syron et al., 2009):

r= $r_{bf\text{-}in}$,

$$D_{Oeff}\frac{dC_O}{dr}=-\left(\frac{P_m*H}{L}\right)\left(\frac{32*P_O}{H}-C_O|r=r_{\ f-in}\right) \quad (18)$$

$$D_{Seff}\frac{dS}{dr}=0 \quad (19)$$

r= $r_{bf\text{-}out}$,

$$D_{Oeff}\frac{dC_O}{dr}=\left(\frac{OW}{L_S}\right)\left(C\ -C|r=r_{\ f-out}\right) \quad (20)$$

$$D_{Seff}\frac{dS}{dr}=\left(\frac{SW}{L_S}\right)\left(S\ -S|r=r_{\ f-out}\right) \quad (21)$$

Where D_{SW} is the substrate diffusivity in water, m^2/s, L_S is the thickness of stagnant layer of liquid, m, D_{OW} is the oxygen diffusivity in water, m^2/s. In modeling studies, the oxygen concentration (C) of liquid phase was added in boundary conditions, which is not included in previous studies.

In order to simplify computations, the linear Finite-Difference Method is introduced. The region is divided into grids. Here, the grid space is uniform, with n+1 points dividing the biofilm thickness into n segments of equal thickness.

The linearization of the non-linear part is as follows: For the equation of oxygen concentration, the following way was used by treating the oxygen in the numerator of the expression as the independent variable, and the oxygen concentrations and the substrate concentration in the denominator as constants. the following linearized expression result is

$$\frac{\mu_m}{K_S + S_{pi}} \frac{S_{pi}}{K_O + C_{pi}} \frac{X_f}{Y_{XO}} C_i$$

Similarly, the equation of substrate concentration was linearized as follows,

$$\frac{\mu_m}{K_S + S_{pi}} \frac{C_{pi}}{K_O + C_{pi}} \frac{X_f}{Y_{XO}} S_i$$

Consequently, the linear system of equations is:

$$D_{Oeff}\left[\frac{C_{i+} - 2C_i + C_{i-}}{h^2} + \left(\frac{1}{r}\right)\frac{C_{i+} - C_{i-}}{2h}\right] - \left[\frac{\mu_m S_{Pi}}{K_S + S_{pi}}\right]\left[\frac{C_i}{K_O + C_{pi}}\right]\frac{X_{bf}}{Y_{XO}} = 0 \qquad (22)$$

$$D_{Seff}\left[\frac{S_{i+} - 2S_i + S_{i-}}{h^2} + \left(\frac{1}{r}\right)\frac{S_{i+} - S_{i-}}{2h}\right] - \left[\frac{\mu_m S_i}{K_S + S_{pi}}\right]\left[\frac{C_{pi}}{K_O + C_{pi}}\right]\frac{X_{bf}}{Y_{XS}} = 0 \qquad (23)$$

where C_{pi} and S_{pi} are the oxygen and substrate concentrations from the previous iteration.

After rearrangement and simplification, the following linear equations are obtained:

$$\frac{o\ ff}{h}\left(\frac{1}{h} + \frac{1}{2(ro+hi)}\right)C_{i+1} + \left(-\frac{2\ o\ ff}{h^2} - \frac{\mu_m S_{p_i}}{K_S + S_{p_i}}\frac{1}{K_O + C_{p_i}}\frac{X_{bf}}{Y_{XO}}\right)C_i + \frac{o\ ff}{h}\left(\frac{1}{h} - \frac{1}{2(ro+hi)}\right)C_{i-1} = 0 \qquad (24)$$

$$\frac{s\ ff}{h}\left(\frac{1}{h}+\frac{1}{2(ro+hi)}\right)S_{i+1}+\left(-\frac{2\ o\ ff}{h^2}-\frac{\mu_m S_{p_i}}{K_S+S_{p_i}}\frac{1}{K_O+C_{p_i}}\frac{X_{bf}}{Y_{XO}}\right)S_i+\frac{s\ ff}{h}\left(\frac{1}{h}-\frac{1}{2(ro+hi)}\right)S_{i-1}=0 \qquad (25)$$

Then, the equations for the elements within the biofilm were identified. That is, for i=1 to n-1, the coefficients to describe oxygen and substrate transport in biofilm are as below.

The coefficients a_{1i}, b_{1i}, C_{1i} and d_{1i} for oxygen in the internal elements are:

$$a_{1i}=-\left(2+\frac{\mu_m}{D_{Oeff}}*\frac{S_{pi}}{K_s+S_{pi}}*\frac{1}{K_O+C_{pi}}*\frac{X_f}{Y_{XO}}*h^2\right)*(r_0+h*i)$$

$$b_{1i}=(r_0+h*i)+\frac{h}{2}$$

$$C_{1i}=(r_0+h*i)-\frac{h}{2}$$

$$d_{1i}=0$$

The coefficientsa_{2i}, b_{2i}, C_{2i} and d_{2i} for substrate in the internal elements are:

$$a_{2i}=-\left(2+\frac{\mu_m}{D_{Seff}}*\frac{1}{K_s+S_{pi}}*\frac{C_{pi}}{K_O+C_{pi}}*\frac{X_f}{Y_{XS}}*h^2\right)*(r_0+h*i)$$

$$b_{2i}=(r_0+h*i)+\frac{h}{2}$$

$$C_{2i}=(r_0+h*i)-\frac{h}{2}$$

$$d_{2i}=0$$

With boundary conditions A:

a) For oxygen when $r = r_{f-in}$, i = 0

$$D_{Oeff}\frac{dC_O}{dr}|r = r_{f-in} = -\left(\frac{P_m * H}{L}\right)\left(\frac{32 * P_O}{H} - C_O|r = r_{f-in}\right) \quad (26)$$

That is

$$Flux = -\left(\frac{P_m * H}{L}\right)\left(\frac{32 * P_O}{H} - C_O|r = r_{f-in}\right)$$

From the previous equation, we can rearrange the items:

$$\left(\frac{P_m * H}{L}\right)\left(\frac{32 * P_O}{H} - C_O\right) * 2\pi r_0 - D_{Oeff} * \frac{(C_o - C)}{dr} * \left(r_0 + \frac{dr}{2}\right) * 2\pi - \left[\left(\mu_m * \frac{S_{po}}{K_S + S_{po}} * \frac{1}{K_O + C_{po}} * \frac{X_{bf}}{Y_{XO}}\right) * 2\pi r_0 * \frac{h}{2}\right] * C_0 = 0 \quad (27)$$

Since $D_{Oeff}\frac{dC_O}{dr}|r = r_{f-in}$,and $C_O|r = r_{f-in}$ is C_O. If i=0, the equation above will change to like follows: Since Flux into biofilm = Flux out of bulk liquid,

$$\left(r_0 + \frac{h}{2}\right) * C_1 - \left[\frac{HP_m}{o\ ff * L} * r_0 * h + \left(r_0 + \frac{h}{2}\right) + \frac{\mu_m}{o\ ff} * \frac{S_{po}}{K_S + S_{po}} * \frac{1}{K_O + C_{po}} * \frac{X_{bf}}{Y_{XO}} * r_0 * \frac{h^2}{2}\right] * C_0 = -\frac{P_m}{o\ ff * L} * 32 * {}_o * r_0 * h \quad (28)$$

the coefficients a_{10}, b_{10}, C_{10} and d_{10} for oxygen in the half-element are:

$$a_{10} = -\left[\frac{H_m}{D_{Oeff} * L_e} * r_0 * h + \left(r_0 + \frac{h}{2}\right) + \frac{\mu_m}{D_{Oeff}} * \frac{S_o}{K_S + S_o} * \frac{1}{K_O + C_o} * \frac{X_{bf}}{Y_{XO}} * r_0 * \frac{h^2}{2}\right]$$

$$b_{10} = r_0 + \frac{h}{2}$$

$$C_{10} = 0$$

$$d_{10} = -\frac{m}{D_{Oeff} * L_e} * 32 * {}_o * r_0 * h$$

b) For substrate when $r = r_{f-in}$, i = 0

$$D_{Seff}\frac{dS}{dr}=0$$

Similarly, the following equation can be achieved:

$$\left(r_0+\frac{h}{2}\right)*S_1-\left[\left(r_0+\frac{h}{2}\right)+\frac{\mu_m}{S\ ff}*\frac{1}{K_S+S_{po}}*\frac{C_{po}}{K_O+C_{po}}*\frac{X_{bf}}{Y_{XS}}*r_0*\frac{h^2}{2}\right]*S_0=0 \qquad (29)$$

Then the coefficients a_{20}, b_{20}, C_{20} and d_{20} for substrate in the half-element:

$$a_{20}=-\left[\left(r_0+\frac{h}{2}\right)+\frac{\mu_m}{D_{Seff}}*\frac{1}{K_S+S_o}*\frac{C_o}{K_O+C_o}*\frac{X_{bf}}{Y_{XO}}*r_0*\frac{h^2}{2}\right]$$

$$b_{20}=r_0+\frac{h}{2}$$

$$C_{20}=0$$

$$d_{20}=0$$

With boundary conditions B:

c) For oxygen when r= r_b, i=n,

$$D_{Oeff}\frac{dC_O}{dr}=\left(\frac{OW}{L_S}\right)\left(C-C|r=r_{f-out}\right) \qquad (30)$$

Similar to those methods used to deal with the boundary-in for the oxygen, the previous equation will change to follows:

$$\left[\left(r-\frac{h}{2}\right)+\frac{OW}{O\ ff}*\frac{h}{ln\left(\frac{b+L}{b}\right)}+\frac{\mu_m}{O\ ff}*\frac{S_{Pn}}{K_S+S_{Pn}}*\frac{1}{K_O+C_{pn}}*\frac{X_{bf}}{Y_{XO}}*r*\frac{h^2}{2}\right]*C_n-\left(r-\frac{h}{2}\right)*C_{n-1}=\frac{OW*C_b*h}{O\ ff*ln\left(\frac{b+L}{b}\right)} \qquad (31)$$

Then the coefficients a_{1n}, b_{1n}, C_{1n} and d_{1n} for oxygen in the half-element at the boundary-

out are:

$$a_{1n} = \left[\left(r_b - \frac{h}{2}\right) + \frac{D_{OW}}{D_{Oeff}} * \frac{h}{ln\left(\frac{r_b + L}{r_b}\right)} + \frac{\mu_m}{D_{Oeff}} * \frac{S_n}{K_S + S_n} * \frac{1}{K_O + C_n} * \frac{X_{bf}}{Y_{XO}} * r_b * \frac{h^2}{2}\right]$$

$$b_{1n} = 0$$

$$C_{1n} = -(r - \frac{h}{2})$$

$$d_{1n} = \frac{D_{OW} * C_b * h}{D_{Oeff} * ln\left(\frac{r_b + L}{r_b}\right)}$$

d) For substrate when r= r_b, i=n,

$$D_{Seff}\frac{dS}{dr} = \left(\frac{SW}{L_S}\right)(S - S|r = r_{f-out})$$

Again, similar to those methods used to deal with the boundary-in for the oxygen, here $S|_{r=r_{bf\text{-}out}}$ is S_n according to previous method the substrate equation can be achieved:

$$\left[\left(r - \frac{h}{2}\right) + \frac{SW}{S_{ff}} * \frac{h}{ln\left(\frac{b+L}{b}\right)} + \frac{\mu_m}{S_{ff}} * \frac{1}{K_S + S_{Pn}} * \frac{C_{pn}}{K_O + C_{pn}} * \frac{X_{bf}}{Y_{XS}} * r * \frac{h^2}{2}\right] * S_n - \left(r - \frac{h}{2}\right) * S_{n-1} = \frac{SW * S_b * h}{S_{ff} * ln\left(\frac{b+L}{b}\right)} \qquad (32)$$

The coefficients a_{2n}, b_{2n}, C_{2n} and d_{2n} for substrate in the internal elements are:

$$a_{2n} = \left[\left(r_b - \frac{h}{2}\right) + \frac{D_{SW}}{D_{Seff}} * \frac{h}{ln\left(\frac{r_b + L}{r_b}\right)} + \frac{\mu_m}{D_{Seff}} * \frac{1}{K_S + S_n} * \frac{C_n}{K_O + C_n} * \frac{X_{bf}}{Y_{XS}} * r_b * \frac{h^2}{2}\right]$$

$$b_{2n} = 0$$

$$C_{2n} = -(r\ -\frac{h}{2})$$

$$d_{2n} = \frac{D_{SW} * S_b * h}{D_{Seff} * ln\left(\frac{r_b + L}{r_b}\right)}$$

Thus, the oxygen and substrate values for i=0 to n have been determined and what need to do is to solve the linear system of equations. Using the assumed initial concentration profiles of the variables as followed:

$$C_{Pi} = C_0 + \left[\frac{C_n - C}{n}\right] * i \qquad (33)$$

$$S_{Pi} = S_0 + \left[\frac{S_n - S}{n}\right] * i \qquad (34)$$

From previous steps of computations, all the coefficients can be collected and three matrixes can be achieved. Then matrix method is introduced.

Where A*B=C, and matrix B is what need to be achieved.

$$A=\begin{bmatrix}
a_{10} & b_{10} & 0 & \cdots & \cdots & \cdots & \cdots & \cdots & 0 & 0 & \cdots & \cdots & \cdots & \cdots & \cdots & 0 \\
c_{11} & a_{11} & b_{11} & 0 & \ddots & 0 & 0 & 0 & \vdots & \vdots & \cdots & \cdots & \cdots & \cdots & \cdots & \vdots \\
0 & c_{12} & a_{12} & b_{12} & 0 & \ddots & 0 & 0 & \vdots & \vdots & \ddots & \ddots & \ddots & \ddots & \ddots & \vdots \\
0 & 0 & c_{13} & a_{13} & b_{13} & 0 & \ddots & 0 & \vdots & \vdots & \ddots & \ddots & \ddots & \ddots & \ddots & \vdots \\
\vdots & \ddots & 0 & \ddots & \ddots & \ddots & 0 & \ddots & \vdots & \vdots & \ddots & \ddots & \ddots & \ddots & \ddots & \vdots \\
\vdots & \ddots & \ddots & 0 & \ddots & \ddots & \ddots & 0 & \vdots & \vdots & \ddots & \ddots & \ddots & \ddots & \ddots & \vdots \\
\vdots & \ddots & \ddots & \ddots & 0 & c_{1n-1} & a_{1n-1} & b_{1n-1} & \vdots & \vdots & \ddots & \ddots & \ddots & \ddots & \ddots & \vdots \\
0 & \cdots & \cdots & \cdots & \cdots & 0 & c_{1n} & a_{1n} & 0 & \cdots & \cdots & \cdots & \cdots & \cdots & \cdots & \vdots \\
0 & \cdots & \cdots & \cdots & \cdots & \cdots & \cdots & 0 & a_{20} & b_{20} & 0 & \cdots & \cdots & \cdots & \cdots & 0 \\
0 & \ddots & \ddots & \ddots & \cdots & \cdots & \cdots & \vdots & c_{21} & a_{21} & b_{21} & 0 & \ddots & \ddots & \ddots & \vdots \\
0 & \ddots & \ddots & \ddots & \cdots & \cdots & \cdots & \vdots & 0 & c_{22} & a_{22} & b_{22} & 0 & \ddots & \ddots & \vdots \\
0 & \ddots & \ddots & \ddots & \cdots & \cdots & \cdots & \vdots & \vdots & \ddots & \ddots & \ddots & \ddots & \ddots & \ddots & \vdots \\
0 & \ddots & \ddots & \ddots & \cdots & \cdots & \cdots & \vdots & \vdots & \vdots & \ddots & \ddots & \ddots & \ddots & \ddots & \vdots \\
0 & \ddots & \ddots & \ddots & \cdots & \cdots & \cdots & \vdots & \vdots & \vdots & \vdots & \ddots & \ddots & \ddots & \ddots & \vdots \\
0 & \ddots & \ddots & \ddots & \ddots & \cdots & \cdots & \vdots & \vdots & \vdots & \vdots & \vdots & \ddots & c_{2n-1} & a_{2n-1} & b_{2n-1} \\
0 & \cdots & \cdots & \cdots & \cdots & \cdots & \cdots & 0 & 0 & \cdots & \cdots & \cdots & 0 & 0 & c_{2n} & a_{2n}
\end{bmatrix}$$

$$B=\begin{bmatrix} C0 \\ C1 \\ C2 \\ \vdots \\ Cn-1 \\ cn \\ S0 \\ S1 \\ S2 \\ \vdots \\ Sn-1 \\ Sn \end{bmatrix} \quad C=\begin{bmatrix} d10 \\ d11 \\ d12 \\ \vdots \\ d1n-1 \\ d1n \\ d20 \\ d21 \\ \vdots \\ d2n-1 \\ d2n \end{bmatrix}$$

According to the calculated concentration profile, MATLAB for iteration is used to find iterative optimization. Based on the numerical experiments about the oxygen concentration profile, a significant difference existed between iteration times of 20 and 40/50 iteration times. As shown in Figure 4, 5, 6, even increased the segments from 50 to 250, the difference trend is similar. However, no significant difference could not be found after 50 times iteration. In order to define the segments value n, the oxygen concentration was tested at same biofilm thickness when segments value changed from 50 to 250 as shown in Table 7. From this Table, no significant difference existed between 150 and 250 segments. The oxygen concentration change in different segments is not significant. Cell size of segments varied from 0.5 to 5 μm and no significant impact of change in cell size in this range was observed. Therefore, an iteration time of 50 and the segments (n) of 200 were used in the modeling studies of this thesis.

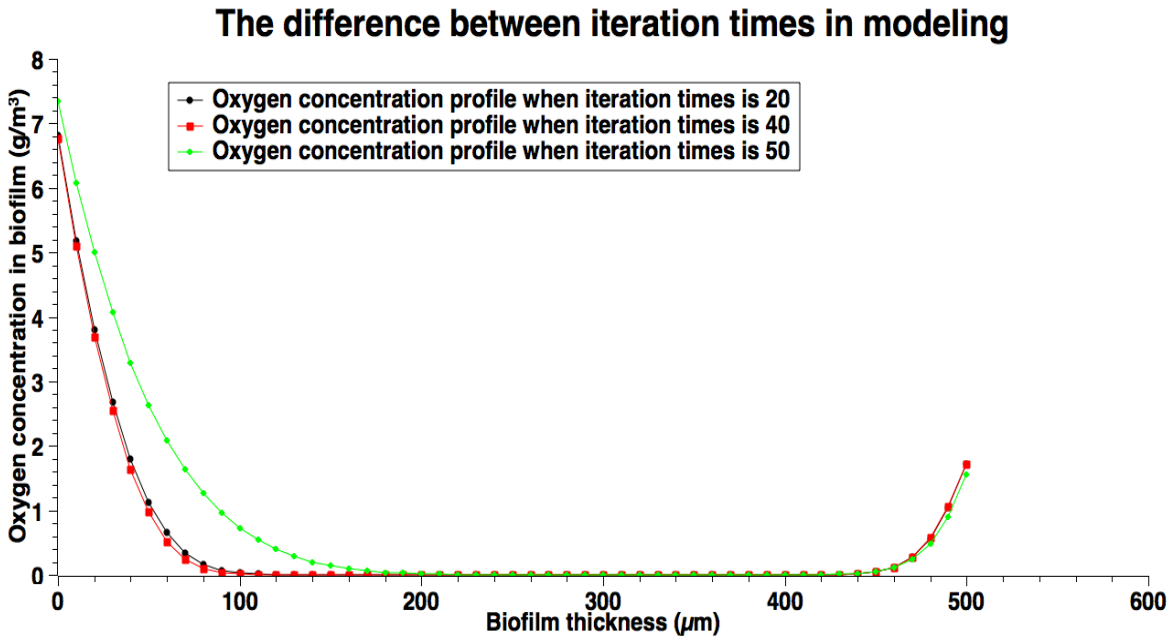

Figure 4. The difference between iteration times when segments are 50

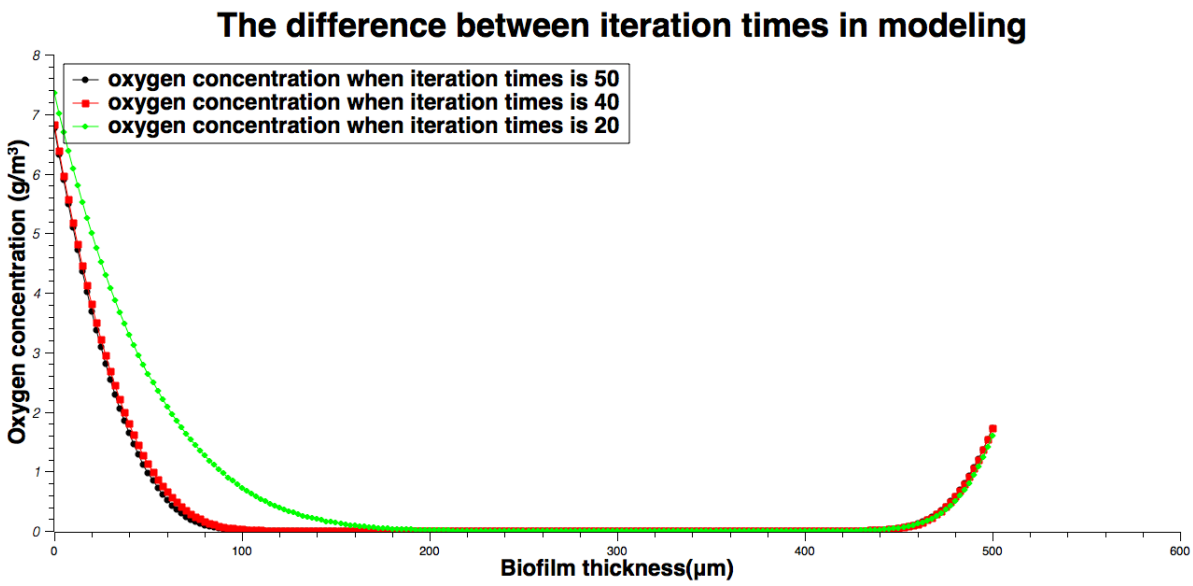

Figure 5. The difference between iteration times when segments are 200

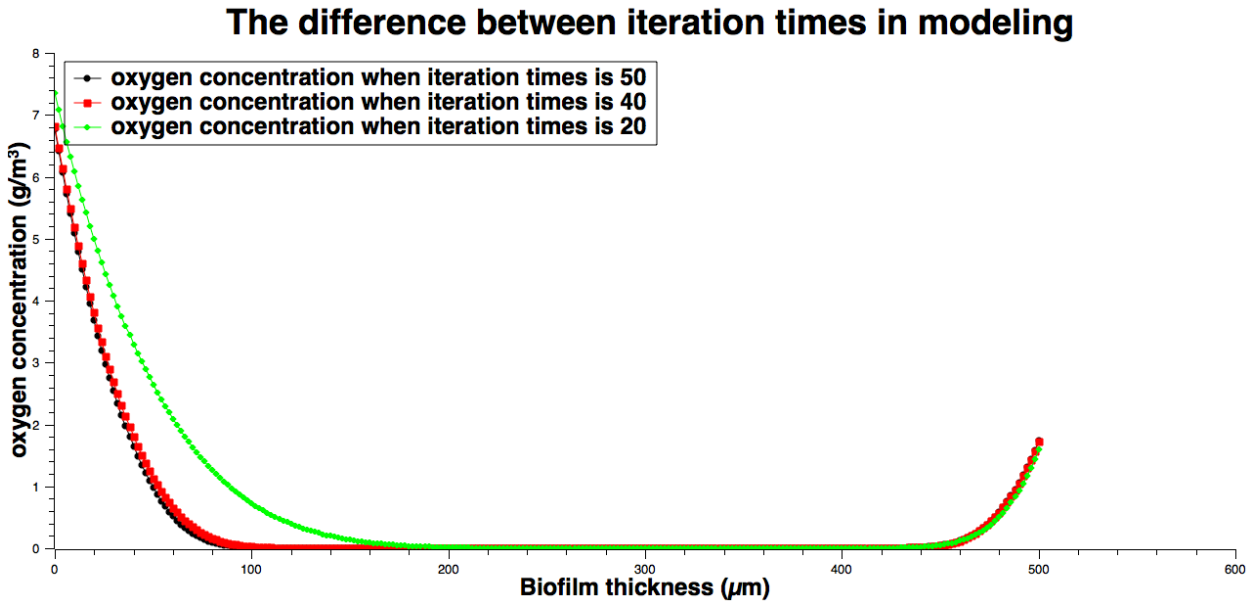

Figure 6. The difference between iteration times when segments are 250

Table 7. The oxygen concentration at the same biofilm thickness with changing segments values

The value of segments (n)	Oxygen concentration at certain biofilm thickness ($20\ \mu m$)	Oxygen concentration at certain biofilm thickness ($100\ \mu m$)	Oxygen concentration at certain biofilm thickness ($400\ \mu m$)	Oxygen concentration at certain biofilm thickness ($1000\ \mu m$)
50	3.0603	1.70E-03	3.23E-18	1.6067
100	3.0778	1.00E-03	1.54E-20	1.6488
150	3.0812	8.33E-04	1.59E-21	1.6587
200	3.0823	8.28E-04	1.46E-21	1.6597
250	3.0828	8.17E-04	1.39E-21	1.6602

The parameters in Table 8 are used to simulate the diffusion and reaction process in the numerical mathematical modeling. These parameters are collected from previous research articles and add them into the modeling study.

Table 8. Parameters for Numerical Modeling of Diffusion and Reaction in Membrane Attached Biofilm, MMABR and ThMABR

Parameters	Symbol	Unit	Typical value MMABR (25℃)	Typical value ThMABR (60℃)
Oxygen diffusivity in biofilm	D_{oeff}	m^2/s	1.6700E-09 (Rittmann et al., 1982)	3.37701E-09 (Richard, 2005)
Substrate diffusivity in biofilm	D_{seff}	m^2/s	1.0000E-09 (Wanner et al., 1994)	2.02216E-09 (Richard, 2005)
Oxygen half-saturation constant	K_O	g/m^3	0.2 (Tanase et al., 2011)	0.2 (Tanase et al., 2011)
Substrate half-saturation constant	K_S	g/m^3	20 (Tanase et al., 2011)	20 (Tanase et al., 2011)
Maximum growth rate	μ_m	1/s	2.3148E-05 (Nicolella et al., 2000)	0.000115741 (Richard, 2005)
Biomass yield based on oxygen	Y_{xo}	/	0.2 (Essila, 1998)	0.2 (Essila, 1998)
Biomass yield based on substrate	Y_{xs}	/	0.45 (Essila, 1998)	0.35 (Richard, 2005)
Biofilm density	X_{bf}	g/m^3	55000 (Essila, 1998)	55000 (Essila, 1998)
Permeability at 25℃	P_m	gmole*m/(m^2*s*atm)	1.6500E-13	2.8100E-13
Effective thickness of hollow fiber membrane	L_e	m	7.5200E-05	7.5200E-05
Stagnant layer of liquid	L_s	m	1.00E-4	1.00E-4
Substrate diffusivity in water	D_{sw}	m^2/s	1.26E-09 (Chen et al., 1988)	2.54792E-09
oxygen diffusivity in water	D_{ow}	m^2/s	2.41E-09 (Tanase et al., 2011)	4.76E-09
Outside radium of hollow fiber membrane	r_0	m	3.18E-04	3.18E-04
Outside radium of biofilm	r_b	m	8.18E-04	8.18E-04
Henry's constant	H	atm*m^3/mole	0.769	1.15761

5. Results and Discussion

Modeling results are organized for discussion in terms of oxygen and substrate concentration profiles, biological activity profiles, membrane-biofilm interfacial oxygen concentration, oxygen penetration distance, and oxygen and substrate fluxes into biofilms under thermophilic and mesophilic conditions.

5.1 Impact of Temperature (thermophilic vs. mesophilic) on oxygen and substrate Concentration Profiles

Figures 7 and 8 showed the concentration profiles of oxygen and substrate within biofilms. The results suggested that the penetration distance of both oxygen and substrate strongly depend on the membrane-biofilm interfacial oxygen concentration. For a low substrate concentration (sb=50 mg/L), substrate transfer is the rate-limiting step; for a medium substrate concentration (sb=100 mg/L), a dual limitation (both oxygen and substrate transfer limitation) is observed in biofilms; for a high substrate concentration (sb=200 mg/L), oxygen transfer is the rate-limiting step. In both situations (thermophilic and mesophilic conditions), substrate either fully or partially penetrates the biofilm, while oxygen always partially penetrates the biofilms.

In most cases for municipal and industrial wastewater treatment, oxygen transfer is the rate-limiting step. Therefore, an increase in interfacial oxygen concentration is required to accommodate biological reactions in biofilms. This can be achieved by using pure oxygen for oxygen transfer. The use of pure oxygen for replacing air can increase the interfacial oxygen concentration and thus increase the penetration distance significantly (Stewart et al., 2016).

Simulating the oxygen and substrate transport process in biofilm can be used to predict the pollutant removal efficiency and oxygen utilization rate. Figure 7 showed the oxygen transport process at different substrate concentration in mesophilic and thermophilic membrane aerated biofilm reactor with air and pure oxygen supplying. The oxygen concentration was up around 2 g/m^3 at the end of biofilm because the air in water layer still would transport into biofilm. The oxygen profile in this simulation is similar to the result of Ntwampe et al., (2008) and Matsumoto et al., (2007).

The oxygen concentration profile in ThMABR system where the substrate concentration had a positive impact on oxygen utilization rate in both biofilm reactors. With increasing substrate concentration, the oxygen utilization rate increased. This increase stimulated the activity of microbial communities on the biofilm which increased the reaction rate. Compared with MMABR, the oxygen concentration in ThMABR system displayed a faster reaction rate and better oxygen utilization rate. The biofilm thickness in ThMABR system is thinner than biofilm in MMABR system as well. This explains why the performance of ThMABR is better than MMABR because thicker biofilms in the millimeter thickness can degrade MMABR performance. These results are also proved the ThMABR system has more advanced points than MMABR system. Thermophilic biofilms were much thinner than mesophilic biofilms, implying operation at thermophilic temperatures could be an effective method to control biofilm thickness (Liao and Liss. 2007).

The substrate concentration both decreased with decreased the biofilm thickness which means the decline substrate utilization rate as biofilm thickness increased (Syron et al.,2009). As shown in Figure 8(a), when the substrate concentration increased to $200g/m^3$, the more significant difference in removal substrate can be found out. It is easy to find more substrate concentration

decrease in ThMABR system. The ThMABR system had a better oxygen utilization performance which supported that the ThMABRs would provide more advanced performance on pollutant removal than the MMABR system.

If the air supplying changed to pure oxygen supplying, the oxygen concentration profiles in different operation conditions were totally similar. The simulated results of ThMABR still showed its outstanding removal abilities, especially for high strength waste water (Figure 8(b)). These results showed increasing oxygen partial pressure would increase reactor performance. It is different from the results from Shanahan and Semmens (2004). In their research, the oxygen partial pressure did not effect on membrane performance.

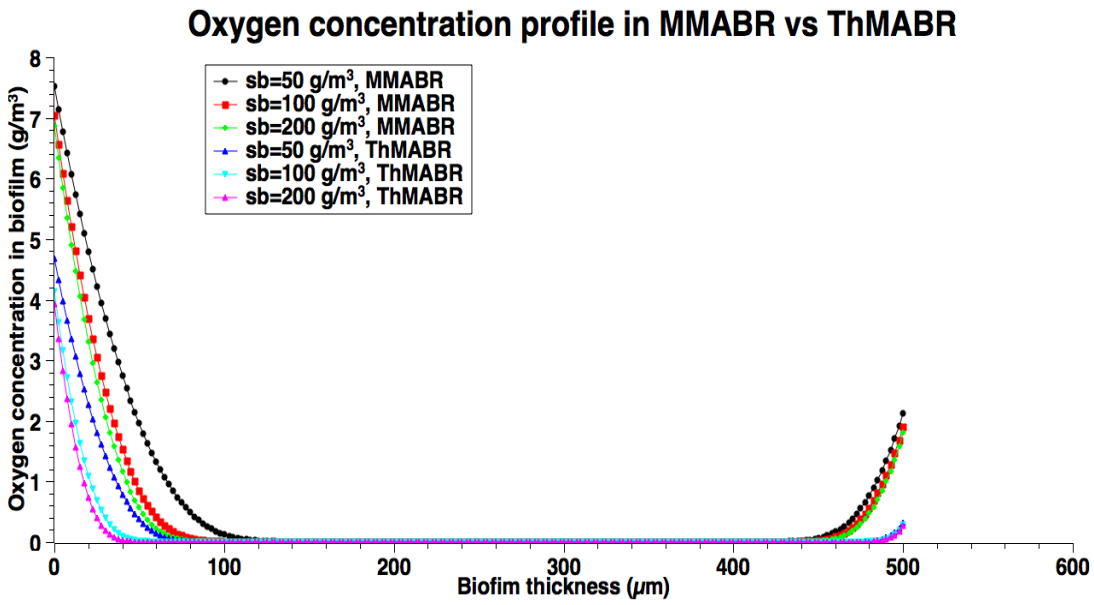

(a)

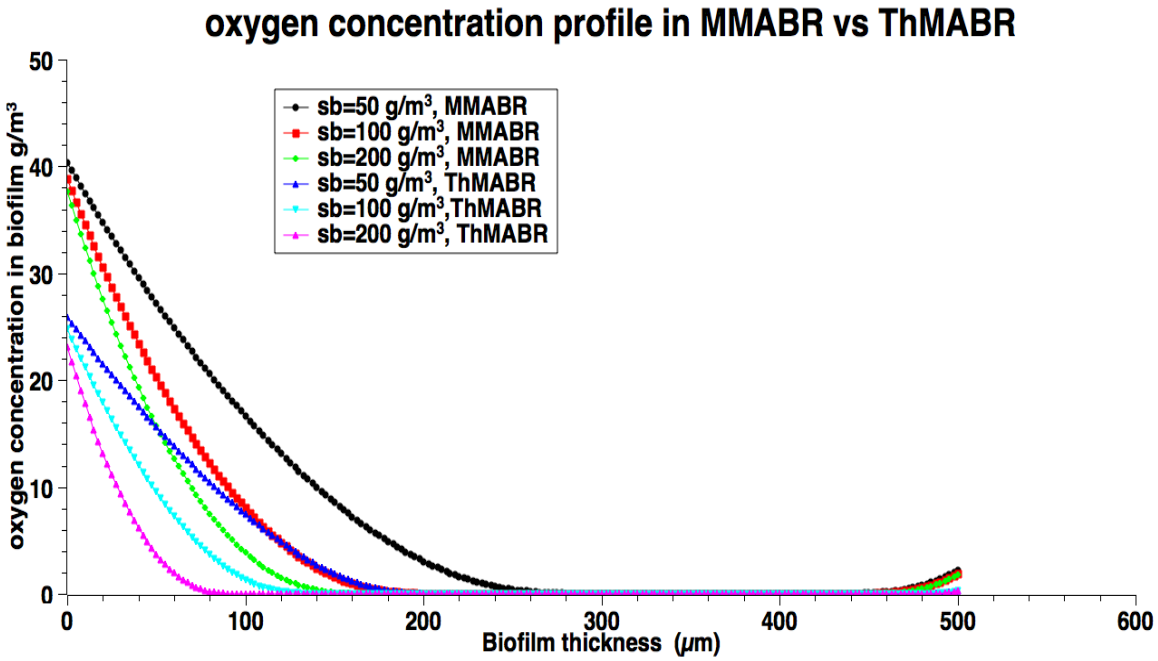

(b)

Figure 7. Oxygen concentration profile in MMABR and ThMABR(a) air supplying (b) pure oxygen supplying

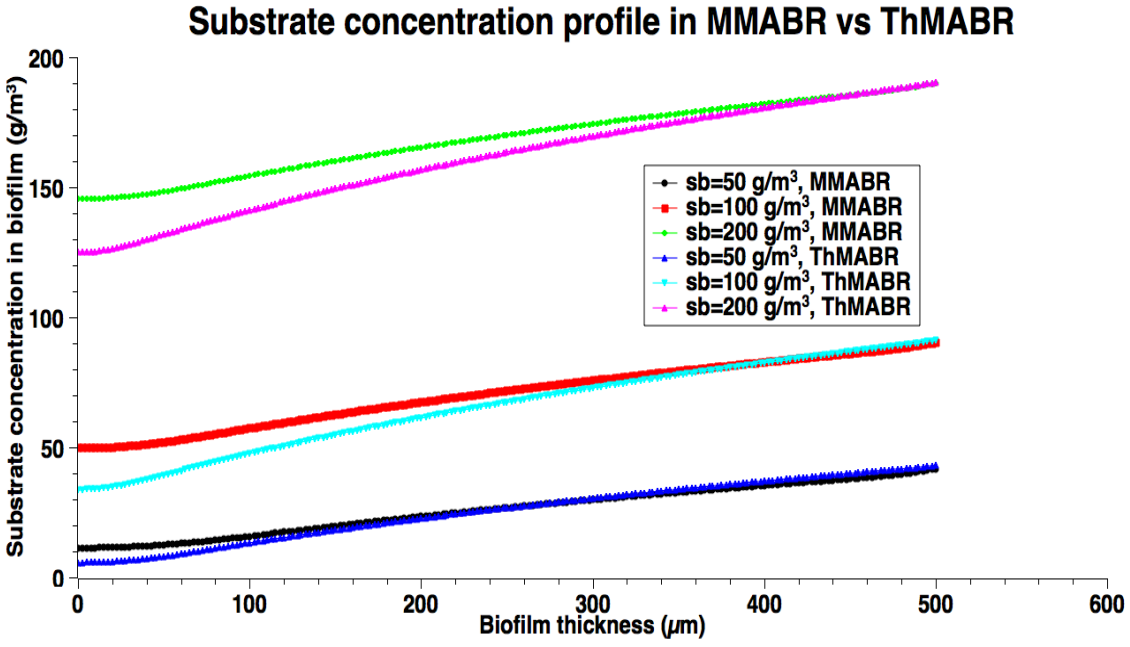

(a)

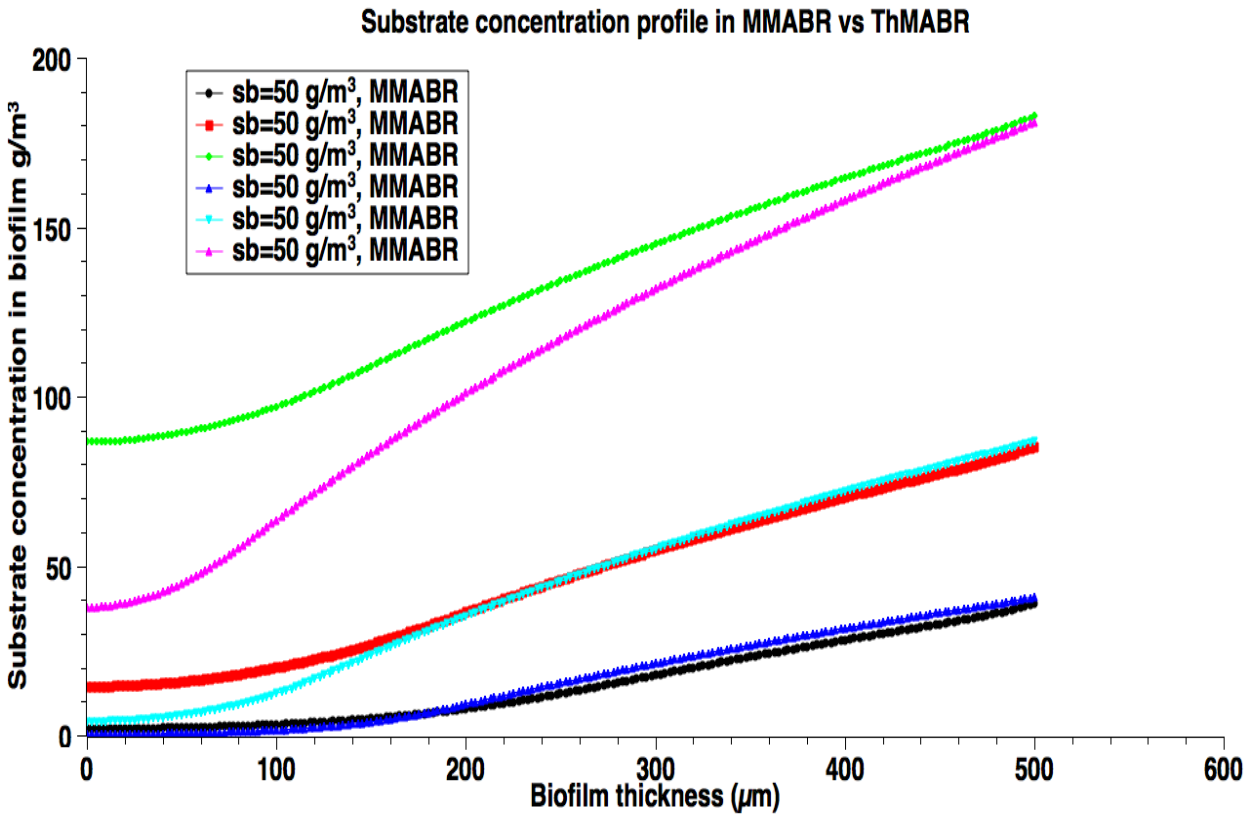

(b)

Figure 8. Substrate concentration profile in ThMABR and MMABR (a) air supplying (b) pure oxygen supplying

5.2 Impact of Temperature on Oxygen Penetration Distance into Biofilms

For high strength wastewater treatment, oxygen transfer is usually the limiting rate step. Therefore, it is important to know the penetration distance of oxygen within biofilms in order to control the biofilm thickness. The penetration distance of oxygen in ThMABR and MMABR is shown in Figure 7(a) and Figure 7(b). The penetration distance of oxygen in MMABR is larger than that in ThMABR. This is probably not surprising, as the interfacial oxygen concentration in MMABR is always higher than that in ThMABRs. In addition, the consumption rate of oxygen

in ThMABRs is higher than that in MMABRs. With substrate concentration increased, the oxygen penetrated into biofilm distance was reduced. As shown in Figure 7(b), when the air was replaced by pure oxygen, the penetration distance of oxygen increased almost double. This phenomenon is similar to Wang et al., (2016). The penetrated distance in MABR was still higher than the distance in ThMABR. These results also indicated the advanced oxygen utilization of ThMABR system.

5.3 Impact of Temperature on Membrane-Biofilm Interfacial Oxygen Concentration

The membrane-biofilm interfacial oxygen concentration is important in determining the penetration distance of oxygen in biofilms. Usually, a high membrane-biofilm interfacial concentration is associated with a larger penetration distance of oxygen in biofilms. A comparison of interfacial oxygen concentration between ThMABR and MMABR is shown in Figure 9. The results suggest that interfacial oxygen concentration in MMABR is higher than that in ThMABR under the similar conditions. Of particular interest is the presence of a minimum interfacial oxygen concentration in terms of biofilm thickness. The presence of the minimum interfacial oxygen concentration may suggest that the presence of an optimal biofilm thickness for a maximum oxygen fluxes into biofilms. When the biofilm thickness is thinner than the optimal biofilm thickness, an increase in biofilm thickness results in an increased consumption of oxygen and thus reduces the interfacial oxygen concentration. When the biofilm thickness is thicker than the optimal biofilm thickness, a further increase in biofilm thickness introduces more transport resistance for both oxygen and substrate and thus reduce the availability of substrate concentration at the membrane-biofilm interface, which corresponds to

an increase in interfacial oxygen concentration. An optimization point of biofilm thickness can be observed in this paper. The profile of interfacial oxygen concentration in both biofilm reactors had a lowest point at certain biofilm thickness which means the highest oxygen flux could be got at an optimal biofilm thickness. It provided a new design idea for future lab scale research.

As shown in Figure 9(b) the use of pure oxygen for replacing air can increase the interfacial oxygen concentration from about 6.5-8 g/m^3 to 36-38 g/m^3 in MMABR system while from 3.75-5.3 g/m^3 to 22-25 g/m^3 in ThMABR system. Thus increase the penetration distance significantly. The use of sealed hollow fibers to deliver oxygen can achieve 100% utilization of oxygen. The optimal biofilm thickness in MMABR is hard to be seen. However, the optimal thickness in ThMABR increased to double. It indicated that using pure oxygen to operate the ThMABR system needs thicker thickness.

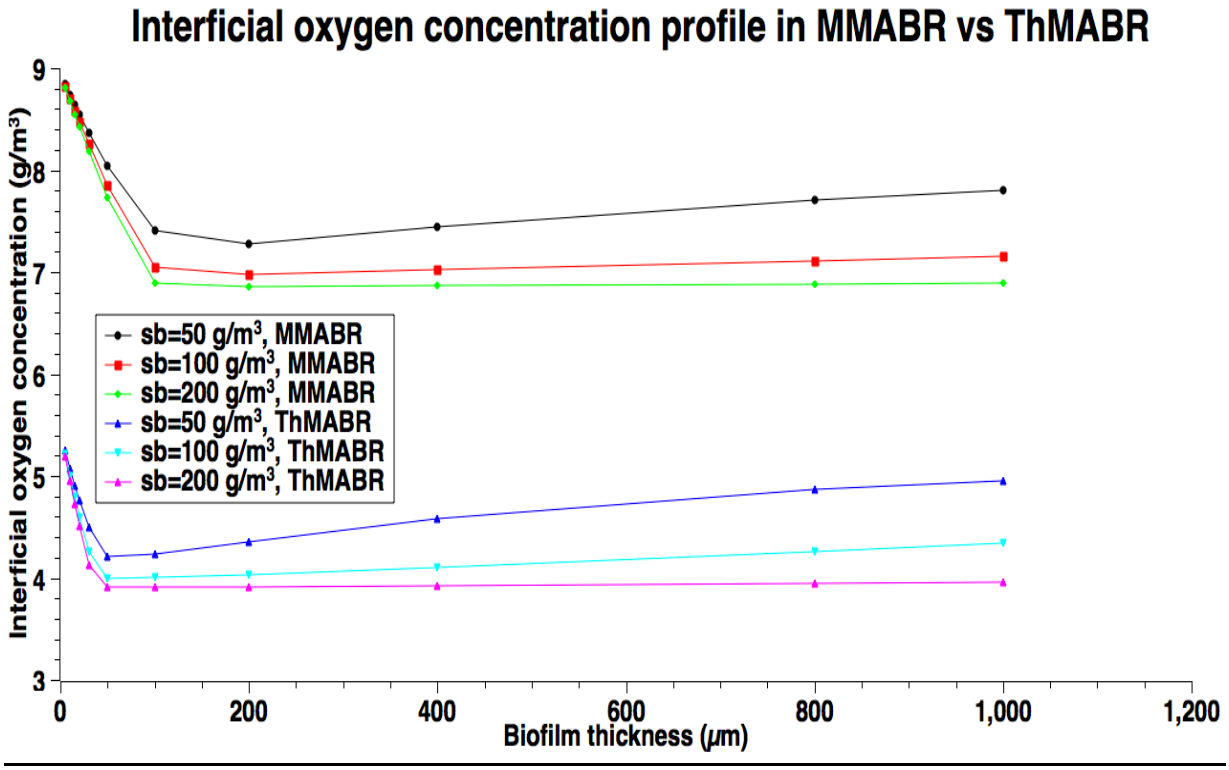

(a)

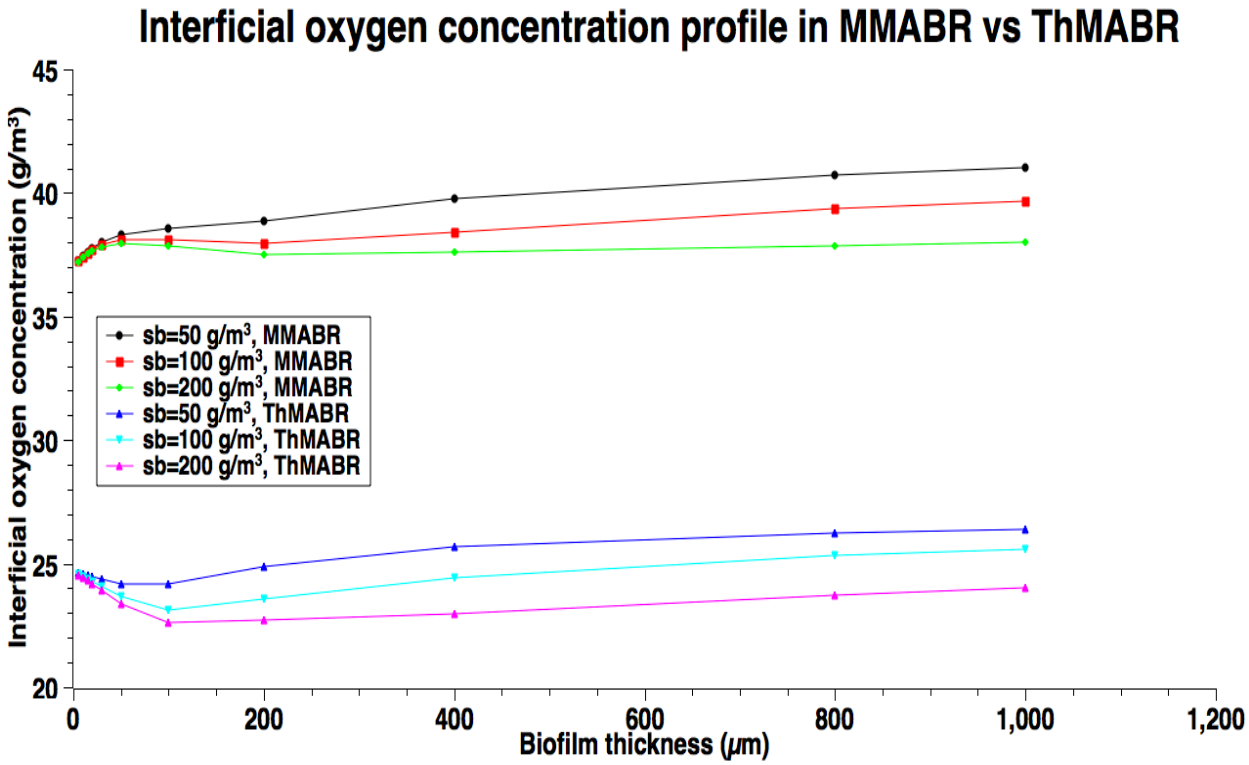

(b)

Figure 9. Interfacial oxygen concentration profile in ThMABR and MMABR (a) air supplying (b) pure oxygen supplying

5.4 Impact of Temperature on Oxygen and Substrate Fluxes into Biofilms

Figure 10 and 11 showed the oxygen and substrate fluxes into biofilm in MMABR and ThMABR, respectively. The results suggest that the presence of a thin layer of biofilm can enhance the flux of oxygen into biofilms. This can be explained by the fact that the presence of a thin layer of biofilm will consume oxygen and thus reduce interfacial oxygen concentration, which leads to an increase in oxygen flux into biofilm. Higher temperatures (thermophilic) increase the transfer of water vapor to the lumen of the hollow fiber membrane and thus increase the water vapor pressure and possible water vapor condensate within the hollow fiber membrane.

The water vapor condensate film in the membrane chamber increases the oxygen mass transfer resistance, thereby reducing the oxygen transfer rate at the thermophilic temperature (Zheng and Liao, 2016). A further increase in biofilm thickness results in a minimum interfacial oxygen concentration, which corresponds to a maximum oxygen flux into biofilm. The result indicates that an optimal biofilm thickness exists for a maximum oxygen flux into biofilms. After the optimal biofilm thickness, any further increase in biofilm thickness will introduce excessive transport resistance for oxygen and substrate transport and thus reduce the oxygen and substrate fluxes into biofilms. The optimal biofilm thickness strongly depends on the intracellular oxygen pressure (Syron and Eoin, 2008).

A comparison of oxygen and substrate fluxes into biofilms between ThMABRs and MMABRs indicates that ThMABRs have advantages over MMABRs in terms of fluxes into biofilms. In a biofilm thickness close to the range of optimal biofilm thickness, the oxygen and substrate fluxes into biofilms in ThMABRs are about 30% higher than that in MMABRs. However, the advantages of fluxes in ThMABRs are reduced when biofilm thickness is further increased. The advantages of fluxes in ThMABRs totally disappear if the biofilm thickness is large enough. These results suggest that a precise control of biofilm thickness at the range of optimal biofilm thickness is essential for achieving the advantages of ThMABRs.

According to Figure 10(b) and Figure 11(b), the pure oxygen increased the peak of oxygen flux which improved substrate fluxes as well. Thus, by increasing the oxygen pressure inside the membranes, we can further increase the flux of oxygen and the substrate removal rate (Motlagh et al, 2006). In the high strength (sb=200 g/m^3) oxygen flux after its peak decreased not significantly in ThMABRs. It also showed thinner biofilm thickness more obviously. In both operation conditions (air and pure oxygen supplying), ThMABRs always displayed advanced

removal abilities for pollutant, which have already been applied in full scale water treatment by their advantages. The thermophilic membrane biofilm system plants have been successfully used for pulp and papermaking wastewater treatment and food processing wastewater treatment. Both systems prove that there are many advantages compared to mesophilic bacteria. Compared to MMABRs, the biological properties of ThMABRs may be better, comparable or worse. The use of ThMABRs for high-temperature industrial wastewater treatment and sludge digestion significantly saves energy and enables energy-neutral or actively processed plants (Duncan et al., 2017).

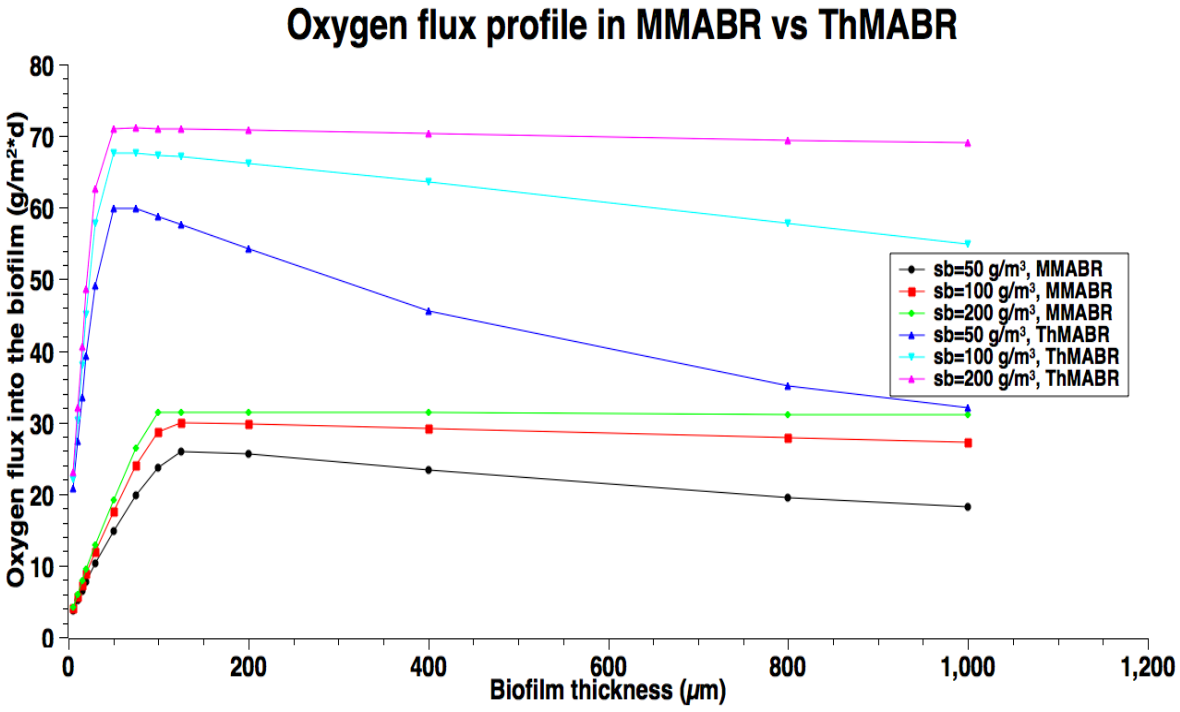

(a)

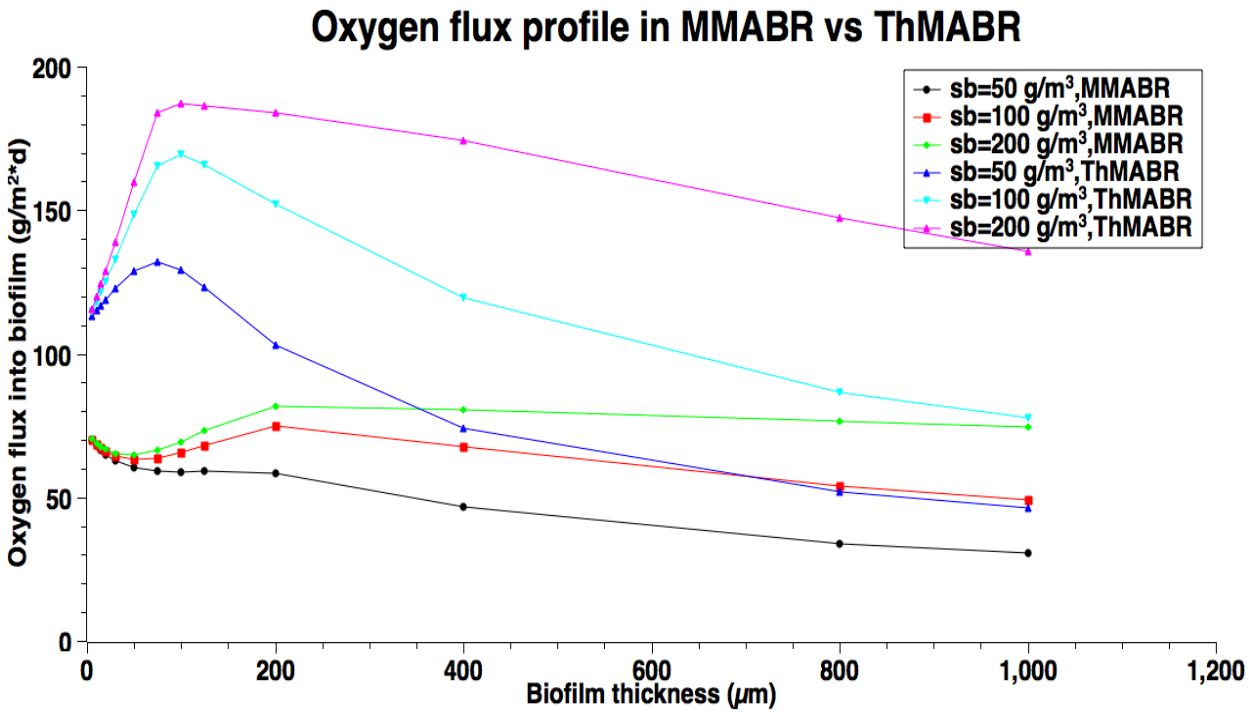

(b)

Figure 10. Oxygen flux comparison on different substrate concentrations (a) air supplying (b) pure oxygen

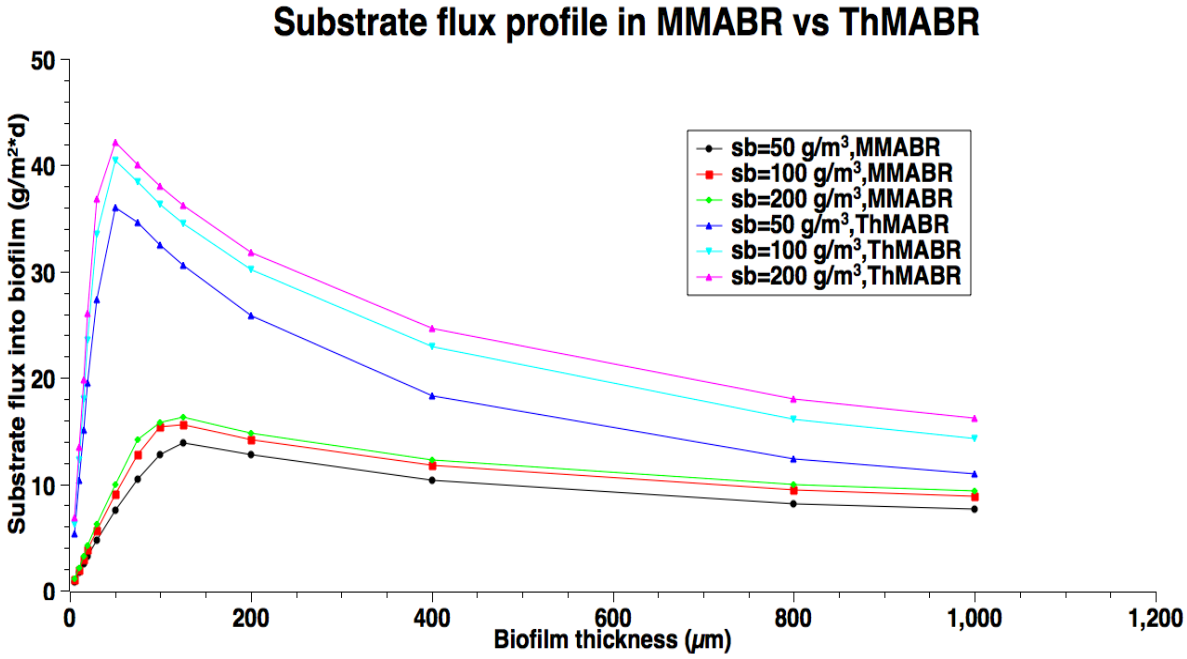

(a)

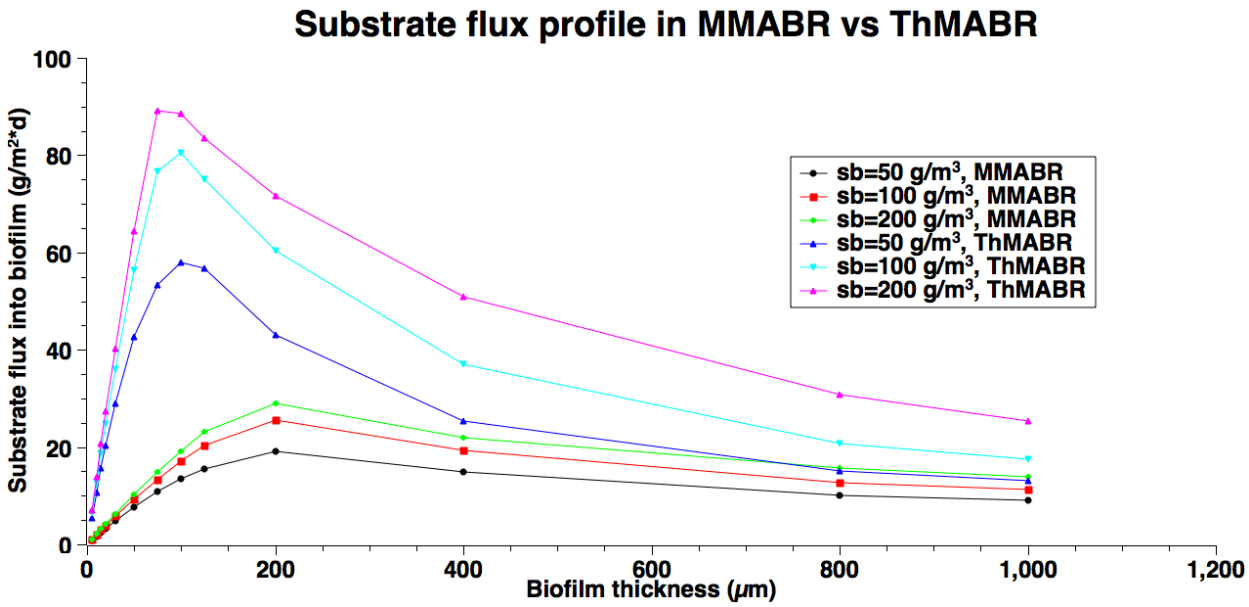

(b)

Figure 11. Substrate flux comparison on different substrate concentrations (a) air supplying (b) pure oxygen supplying

5.5 Case study

This numerical model provides detailed results of diffusion and reaction processes in biofilm. However, in order to maximize the modeling results effectively, it can be used to compare the modeling results with the experimental results and examine the overall impact of reactor design and biofilm properties and operating conditions on overall MABR performance.

Liao and Liss (2007) found out that MABR running at a thermophilic temperature (55 ^{o}C) (ThMABR) was more effective than MMABR in COD removal and biofilm thickness control for a synthetic high-strength organic wastewater treatment. The COD (feed COD concentration was 1200 mg/L) removal process can be simulated by this mathematical modeling. Based on the membrane properties (hollow fiber silicone Model: M60-130W-200L-FC8, 13 cm wide x 20 cm long, supplied by Nagayanagi Co., Ltd., Japan; outer diameter 320 μm; inner diameter: 200 μm;

8 layers and 1600 fibers per module; total surface area: 0.26 m^2; specific surface area: 173.3 m^2/m^3) and biofilm thickness of 1080 μm and 280 μm for MMABR and ThMABR, respectively (Liao and Liss. 2007), and the modeling results are summarized in Table 9 and compared to the experimental results.

At an air gauge pressure of 4 and 6 psi, the substrate fluxes into the MMABR was 9.9223 and 10.179 g/m^2*d, while the substrate fluxes into the ThMABR was 33.05 and 34.91 g/m^2*d, respectively. Similarly, the oxygen fluxes were 38.03 and 40.57 g/m^2*d for MMABR and 87.37 and 93.49 g/m^2*d at an air gauge pressure of 4 and 6 psi, respectively. The results showed that an increase in the oxygen partial pressure led to an improved COD removal efficiency. These results clearly showed the advantages of the ThMABR system. This system showed a higher substrate flux or COD removal in both the modeling and experimental results. Thermophilic biofilms were much thinner than mesophilic biofilms, which implied that operating at thermophilic temperatures might be an effective approach of controlling biofilm thickness. This explains why the ThMABR performed better than the MMABR because a thicker biofilm in the millimeter thickness range deteriorated the performance of the MMABR. Similarly, when the oxygen pressure changed to 6psi, the substrate flux was still higher than the flux in the MMABR system. According to the experimental results, the simulated results are reasonable. The pollutant removal efficiency of ThMABR is higher than the removal in MMABR. The experimental results from the literature (Liao and Liss, 2007) verified that the general trend of the higher COD removal efficiency in the ThMABR system. The difference between the modeled results and experimental results could be at least partially caused by the back diffusion of water vapor into the lumen side of the hollow fibers, which caused additional mass transfer resistance of oxygen to biofilm. It was noted that much more water condensate was observed from the ThMABR

system, due to the higher back diffusion of water vapor at the thermophilic temperature. It is suggested to design a vertical module to reduce the water condensate accumulation by flowing out the lumen by gravity, rather than the use of a horizontal membrane module as used by Liao and Liss (2007). Furthermore, the MABR systems used by Liao and Liss were sequencing batch MABRs. The effluent concentration was measured after 24 hours reaction. However, for the ThMABR system, the lower effluent COD (around 100 mg/L) could be achieved in less than 24 hours. In that case, the reaction cyclic time could be significantly reduced for the ThMABR system and thus increased the COD removal rate significantly, which would eventually lead to a closer value of COD removal rate between modeling and experimental studies for the ThMABR system.

Table 9. The oxygen and substrate flux into biofilm under different air gauge pressures

Biofilm reactor	Oxygen flux (g/m^2*d)	Substrate flux(g/m^2*d)	Simulate COD removal rate (g/d)	Experiment COD removal rate (g/d)
MMABR (25℃, 4psi)	38.0287	9.9223	2.5780	1.1625
MMABR (25℃, 6psi)	40.5721	10.1794	2.6466	1.2375
ThMABR (55℃, 4psi)	87.3721	33.0497	8.5929	1.6532
ThMABR (55℃, 6psi)	93.4913	34.9091	9.0763	1.6826

6. Conclusions

The concept of ThMABR was proposed for high strength wastewater and gas treatments. Theoretical analyses and modeling were conducted to elucidate the advantages and disadvantages compared to MMABR. The main conclusions are drawn below:

1.) An increase in temperature from the mesophilic to the thermophilic range results in a significant increase in the oxygen and substrate fluxes into biofilms. The oxygen and substrate flux into biofilms at 60^{o}C is about much higher than that at 25^{o}C, respectively.

2.) Under similar operating conditions, oxygen penetration distance of ThMABRs is smaller than that of the MMABRs, implying the control of biofilm thickness in ThMABRs is even more important than in MMABRs.

3.) Under similar operating conditions, membrane-biofilm interfacial oxygen concentration in ThMABRs is lower than that in MMABRs.

4.) The effect of increasing the temperature demonstrates that thermophilic MABRs are superior to mesophilic MABRs in treating high strength wastewater and gases, even increasing the partial pressure of oxygen.

7. Future studies

The mathematical modeling established in this thesis is one-dimensional model. In order to further research the thermophilic MABR systems performance and applications, the future works may include two-dimensional or three-dimensional modeling establishing. Furthermore,

experimental studies should be conducted to further verify the findings of the theoretical modeling from this study.

Abbreviations

HRT	hydraulic retention time (h)
AOB	ammonia-oxidizing bacteria
NOB	nitrite-oxidizing bacteria
SRT	sludge retention time (d)
HB	heterotrophic bacteria
SBMABR	sequencing batch membrane-aerated biofilm reactor
CMABR	carbon membrane-aerated biofilm reactor
MMABR	mesophilic membrane aerated biofilm reactor
ThMABR	thermophilic membrane aerated biofilm reactor
TABT	thermophilic aerobic biological treatment
M2BR	membrane-coupled bioreactor
AS-MBR	activated sludge membrane separation reactor
PVDF	polyvinylidene fluoride
PDMS	polydimethylsiloxane
GRT	gas residence time (s)
EBRT	empty bed residence time (s)
J	flux (g/m^2*d)
K_{la}	overall mass transfer coefficient (min^{-1})
r_c	substrate consumption rate (1/s)
T	absolute temperature of liquid under testing (°K)
K	proportionality constant
E	modulus of elasticity of water at temperature T, (kNm^{-2})
μ	dynamic viscosity of the solvent
ρ	density of water at temperature T, ($kg\ m^{-3}$)
σ	interfacial surface tension of water at temperature T, ($N\ m^{-1}$)
P_s	saturation pressure at the equilibrium position (atm).
Ko	oxygen half-saturation constant (mg/L)
Ks	substrate half-saturation constant (mg/L)
	Sutherland constant
H	henry's constant ($atm*m^3/mole$)
$\mu(w)$	viscosity of water (Pa·s)
$\mu(g)$	viscosity of gas (Pa·s)
S_{O_g}	oxygen solubility in gas phase (g/L)
S_{O_w}	oxygen solubility in liquid phase (g/L)
P_{O_g}	oxygen permeability in PDMS membrane ($gmole*m/(m^2*s*atm)$
D_w	diffusion coefficient in water (m^2/s)
D_{AB}	diffusion coefficient in air (m^2/s)

ε	porosity of biofilms
τ	tortuosity factor
COD	chemical oxygen demand
μ_m	maximum growth rate (1/s)
Yxo	biomass yield based on oxygen
Yxs	biomass yield based on substrate
Xbf	biofilm density (g/m^3)
P_m	permeability at 25℃ (gmole*m/(m^2*s*atm)
L_e	effective thickness of hollow fiber membrane (m)
L_s	stagnant layer of liquid (m)
D_{sw}	substrate diffusivity in water (m^2/s)
D_{ow}	oxygen diffusivity in water (m^2/s)
r_0	outside radium of hollow fiber membrane (m)
r_b	outside radium of biofilm (m)
D_{eff}	effective diffusivity of oxygen in membrane (m^2/s)

REFERENCES

Ahmad, I., Ahmad, F., & Pichtel, J. (Eds.). (2011). Microbes and microbial technology: agricultural and environmental applications. Springer Science & Business Media.

Ahmed, T., Semmens, M. J., & Voss, M. A. (2004). Oxygen transfer characteristics of hollow-fiber, composite membranes. *Advances in Environmental Research*, *8*(3-4), 637-646.

Ahmed, Z., Cho, J., Lim, B. R., Song, K. G., & Ahn, K. H. (2007). Effects of sludge retention time on membrane fouling and microbial community structure in a membrane bioreactor. Journal of membrane science, 287(2), 211-218.

Al-Shemmeri. T. (2012). Engineering Fluid Mechanics, Ventus Publishing ApS,.

Álvarez-Hornos, F. J., Volckaert, D., Heynderickx, P. M., & Van Langenhove, H. (2011). Performance of a composite membrane bioreactor for the removal of ethyl acetate from waste air. Bioresource technology, 102(19), 8893-8898

Álvarez-Hornos, F. J., Volckaert, D., Heynderickx, P. M., & Van Langenhove, H. (2012). Removal of ethyl acetate, n-hexane and toluene from waste air in a membrane bioreactor under continuous and intermittent feeding conditions. Journal of Chemical Technology and Biotechnology, 87(6), 739-745.

Baek, S. H., & Pagilla, K. R. (2008). Simultaneous nitrification and denitrification of municipal wastewater in aerobic membrane bioreactors. Water Environment Research, 80(2), 109-117.

Cao, C., Zhao, L., Xu, D., & Geng, Q. I. J. I. N. (2009). Membrane-Aerated Biofilm Reactor Behaviors for the Treatment of High-Strength Ammonium Industrial Wastewater." Chemical engineering & technology32(4), 613-621.

Casey, E. (2007). Simulation studies of process scale membrane aerated biofilm reactor configurations. In 4th International Water Association Membranes Conference, Harrogate, UK

Casey, E., Glennon, B., & Hamer, G. (1999). Review of membrane aerated biofilm reactors. Resources, conservation and recycling, 27(1-2), 203-215.

Casey, E., Syron, E., Shanahan, J. W., & Semmens, M. J. (2008). Comparative economic analysis of full scale mabr configurations. In 2008 IWA North American Membrane Research Conference, University of Massachusetts, Amherst, USA, August 10-13, 2008.

Chen, G. H., Hiroaki Ozaki, and Yutaka Terashima. (1988). Modelling of the simultaneous removal of organic substances and nitrogen in a biofilm. Water Pollution Research and Control Brighton. 791-804.

Chen, R. D., Semmens, M. J., & LaPara, T. M. (2008). Biological treatment of a synthetic space mission wastewater using a membrane-aerated, membrane-coupled bioreactor (M2BR). Journal of industrial microbiology & biotechnology, 35(6), 465-473.

Choi, J., Kim, E. S., & Ahn, Y. (2017). Microbial community analysis of bulk sludge/cake layers and biofouling-causing microbial consortia in a full-scale aerobic membrane bioreactor. Bioresource technology, 227, 133-141.

Collivignarelli, M. C., Castagnola, F., Sordi, M., & Bertanza, G. (2015). Treatment of sewage sludge in a thermophilic membrane reactor (TMR) with alternate aeration cycles. Journal of environmental management, 162, 132-138.

District, S. R. C. S. (2009). Ammonia Removal Options for High Purity Oxygen Activated Sludge Systems: a Literature Review.

Dong, W. Y., Wang, H. J., Li, W. G., Ying, W. C., Gan, G. H., & Yang, Y. (2009). Effect of DO on simultaneous removal of carbon and nitrogen by a membrane aeration/filtration combined bioreactor. Journal of Membrane Science, 344(1), 219-224.

Downing, L. S., & Nerenberg, R. (2008). Effect of bulk liquid BOD concentration on activity and microbial community structure of a nitrifying, membrane-aerated biofilm. Applied microbiology and biotechnology, 81(1), 153-162.

Downing, L. S., & Nerenberg, R. (2008). Total nitrogen removal in a hybrid, membrane-aerated activated sludge process. Water research, 42(14), 3697-3708.

Duncan, J., Bokhary, A., Fatehi, P., Kong, F., Lin, H., & Liao, B. Thermophilic membrane bioreactors: A review. Bioresource technology 243 (2017): 1180-1193.

Essilia. N.J. (1997). Contrasting behaviour of biofilms grown on gas permeable membranes with those grown on solid surfaces: a model study, M.Sc. Thesis, University of Minnisota, USA.

Furumai, H., and Rittmann, B. E. (1992). Advanced modeling of mixed populations of heterotrophs and nitrifiers considering the formation and exchange of soluble microbial products.Water Sci. and Technol., 26(3-4), 493-502

Feng, Y. J., Tseng, S. K., Hsia, T. H., Ho, C. M., & Chou, W. P. (2007). Partial nitrification of ammonium-rich wastewater as pretreatment for anaerobic ammonium oxidation (Anammox) using membrane aeration bioreactor. Journal of bioscience and bioengineering, 104(3), 182-187.

Feng, Y. J., Tseng, S. K., Hsia, T. H., Ho, C. M., & Chou, W. P. (2008). Aerated membrane-attached biofilm reactor as an effective tool for partial nitrification in pretreatment of anaerobic ammonium oxidation (ANAMMOX) process. Journal of chemical technology and biotechnology, 83(1), 6-11.

Gilmore, K. R., Terada, A., Smets, B. F., Love, N. G., & Garland, J. L. (2013). Autotrophic nitrogen removal in a membrane-aerated biofilm reactor under continuous aeration: a demonstration. Environmental Engineering Science, 30(1), 38-45.

Gong, Z., Liu, S., Yang, F., Bao, H., & Furukawa, K. (2008). Characterization of functional microbial community in a membrane-aerated biofilm reactor operated for completely autotrophic nitrogen removal. Bioresource Technology, 99(8), 2749-2756.

Gong, Z., Yang, F., Liu, S., Bao, H., Hu, S., & Furukawa, K. (2007). Feasibility of a membrane-aerated biofilm reactor to achieve single-stage autotrophic nitrogen removal based on Anammox. Chemosphere, 69(5), 776-784.
Hasar, H., Xia, S., Ahn, C. H., & Rittmann, B. E. (2008). Simultaneous removal of organic matter and nitrogen compounds by an aerobic/anoxic membrane biofilm reactor. water research, 42(15), 4109-4116.
Hou, F., Li, B., Xing, M., Wang, Q., Hu, L., & Wang, S. (2013). Surface modification of PVDF hollow fiber membrane and its application in membrane aerated biofilm reactor (MABR). Bioresource technology, 140, 1-9.
Hu, L., Liu, B., Li, B., Hou, F., Wang, Q., Zhang, H., ... & Lian, M. (2016). Investigation of membrane-aerated biofilm reactor (MABR) for the treatment of crude oil wastewater from offshore oil platforms. Desalination and Water Treatment, 57(9), 3861-3870.
Iorhemen, O. T., Hamza, R. A., & Tay, J. H. (2016). Membrane bioreactor (MBR) technology for wastewater treatment and reclamation: membrane fouling. Membranes, 6(2), 33.
Jiang, X., Xu, B., & Wu, J. (2018). Sulfur recovery in the sulfide-oxidizing membrane aerated biofilm reactor: experimental investigation and model simulation. Environmental technology, 1-11.
Juteau, P. (2006). Review of the use of aerobic thermophilic bioprocesses for the treatment of swine waste. Livestock Science, 102(3), 187-196.
Kumar, A., Chilongo, T., Dewulf, J., Ergas, S. J., & Van Langenhove, H. (2010). Gaseous dimethyl sulphide removal in a membrane biofilm reactor: effect of methanol on reactor performance. Bioresource technology, 101(23), 8955-8959.
Kumar, A., Dewulf, J., & Van Langenhove, H. (2008). Membrane-based biological waste gas treatment. Chemical Engineering Journal, 136(2), 82-91.
Kumar, A., Dewulf, J., Luvsanjamba, M., & Van Langenhove, H. (2008). Continuous operation of membrane bioreactor treating toluene vapors by Burkholderia vietnamiensis G4. Chemical Engineering Journal, 140(1), 193-200.
Kumar, A., Dewulf, J., Vercruyssen, A., & Van Langenhove, H. (2009). Performance of a composite membrane bioreactor treating toluene vapors: inocula selection, reactor performance and behavior under transient conditions. Bioresource technology, 100(8), 2381-2387.
Lackner, S., Terada, A., & Smets, B. F. (2008). Heterotrophic activity compromises autotrophic nitrogen removal in membrane-aerated biofilms: results of a modeling study. Water research, 42(4), 1102-1112.
Lackner, S., Terada, A., Horn, H., Henze, M., & Smets, B. F. (2010). Nitritation performance in membrane-aerated biofilm reactors differs from conventional biofilm systems. Water research, 44(20), 6073-6084.
LaPara, T. M., Nakatsu, C. H., Pantea, L., & Alleman, J. E. (2000) Phylogenetic analysis of bacterial communities in mesophilic and thermophilic bioreactors treating pharmaceutical wastewater. Applied and environmental microbiology 66.9: 3951-3959.
LaPara, T. M., and James E. Alleman. (1999). Thermophilic aerobic biological wastewater treatment."Water Research33.4: 895-908.
Lebrero, R., Gondim, A. C., Pérez, R., García-Encina, P. A., & Muñoz, R. (2014). Comparative assessment of a biofilter, a biotrickling filter and a hollow fiber membrane bioreactor for odor treatment in wastewater treatment plants. Water research, 49, 339-350.
Lebrero, R., Volckaert, D., Pérez, R., Muñoz, R., & Van Langenhove, H. (2013). A membrane bioreactor for the simultaneous treatment of acetone, toluene, limonene and hexane at trace level concentrations. Water research, 47(7), 2199-2212.
Li, M., Li, P., Du, C., Sun, L., & Li, B. (2016). Pilot-Scale Study of an Integrated Membrane-Aerated Biofilm Reactor System on Urban River Remediation. Industrial & Engineering Chemistry Research, 55(30), 8373-8382.
Li, P., Li, M., Zhang, Y., Zhang, H., Sun, L., & Li, B. (2016). The treatment of surface water with enhanced membrane-aerated biofilm reactor (MABR). Chemical Engineering Science, 144, 267-274.
Li, P., Zhao, D., Zhang, Y., Sun, L., Zhang, H., Lian, M., & Li, B. (2015). Oil-field wastewater treatment by hybrid membrane-aerated biofilm reactor (MABR) system. Chemical Engineering Journal, 264, 595-602.
Li, Shiyu, and Guang Hao Chen. (1994) Modeling the organic removal and oxygen consumption by biofilms in an open-channel flow.Water Science and Technology 30.2: 53-61.
Li, T., Bai, R., & Liu, J. (2008). Distribution and composition of extracellular polymeric substances in membrane-aerated biofilm. Journal of Biotechnology, 135(1), 52-57.
Li, T., Liu, J., Bai, R., & Wong, F. S. (2008). Membrane-aerated biofilm reactor for the treatment of acetonitrile wastewater. Environmental science & technology, 42(6), 2099-2104.
Li, X., Sun, S., Badgley, B. D., Sung, S., Zhang, H., & He, Z. (2016). Nitrogen removal by granular nitritation–anammox in an upflow membrane-aerated biofilm reactor. Water research, 94, 23-31.
Li, Y., & Zhang, K. (2018). Pilot scale treatment of polluted surface waters using membrane-aerated biofilm reactor (MABR). Biotechnology & Biotechnological Equipment, 32(2), 376-386.
Liao, B. Q., & Liss, S. N. (2007). A comparative study between thermophilic and mesophilic membrane aerated biofilm reactors. Journal of Environmental Engineering and Science, 6(2), 247-252.
Liao, B. Q., Zheng, M. R., & Ratana-Rueangsri, L. (2010). Treatment of synthetic kraft evaporator condensate using thermophilic and mesophilic membrane aerated biofilm reactors. Water Science and Technology, 61(7), 1749-1756.
Lin, J., Zhang, P., Li, G., Yin, J., Li, J., & Zhao, X. (2016). Effect of COD/N ratio on nitrogen removal in a membrane-aerated biofilm reactor. International Biodeterioration & Biodegradation, 113, 74-79.
Lin, J., Zhang, P., Yin, J., Zhao, X., & Li, J. (2015). Nitrogen removal performances of a polyvinylidene fluoride membrane-aerated biofilm reactor. International Biodeterioration & Biodegradation, 102, 49-55.

Liu, C., Xiao, T. M., Zhang, J., Zhang, L., Yang, J. L., & Zhang, M. (2014). Effect of membrane wettability on membrane fouling and chemical durability of SPG membranes used in a microbubble-aerated biofilm reactor. Separation and Purification Technology, 127, 157-164.
Liu, H., Tan, S., Sheng, Z., Liu, Y., & Yu, T. (2014). Bacterial community structure and activity of sulfate reducing bacteria in a membrane aerated biofilm analyzed by microsensor and molecular techniques. Biotechnology and bioengineering, 111(11), 2155-2162.
Liu, H., Yang, F., Shi, S., & Liu, X. (2010). Effect of substrate COD/N ratio on performance and microbial community structure of a membrane aerated biofilm reactor. Journal of Environmental Sciences, 22(4), 540-546.
Liu, H., Yang, F., Wang, T., Liu, Q., & Hu, S. (2007). Carbon membrane-aerated biofilm reactor for synthetic wastewater treatment. Bioprocess and biosystems engineering, 30(4), 217-224.
Liu, Y., Ngo, H. H., Guo, W., Peng, L., Pan, Y., Guo, J., ... & Ni, B. J. (2016). Autotrophic nitrogen removal in membrane-aerated biofilms: Archaeal ammonia oxidation versus bacterial ammonia oxidation. Chemical Engineering Journal, 302, 535-544.
López, L. G., Veiga, M. C., Nogueira, R., Aparicio, A., & Melo, L. F. (2003). A technique using a membrane flow cell to determine average mass transfer coefficients and tortuosity factors in biofilms. Water Science and Technology47.5: 61-67.
Luvsanjamba, M., Kumar, A., & Van Langenhove, H. (2008). Removal of dimethyl sulfide in a thermophilic membrane bioreactor. Journal of chemical technology and biotechnology, 83(9), 1218-1225.
Matsumoto, S., Terada, A., & Tsuneda, S. (2007). Modeling of membrane-aerated biofilm: effects of C/N ratio, biofilm thickness and surface loading of oxygen on feasibility of simultaneous nitrification and denitrification. Biochemical Engineering Journal, 37(1), 98-107.
Matsumoto, Shinya, Akihiko Terada, and Satoshi Tsuneda. (2007). Modeling of membrane-aerated biofilm: effects of C/N ratio, biofilm thickness and surface loading of oxygen on feasibility of simultaneous nitrification and denitrification. Biochemical Engineering Journal 37.1: 98-107.
Mclamore, E. S., Zhang, W., Porterfield, D. M., & Banks, M. K. (2010). Membrane-aerated biofilm proton and oxygen flux during chemical toxin exposure. Environmental science & technology, 44(18), 7050-7057.
McLamore, E., Jackson, W. A., & Morse, A. (2007). Abiotic transport in a membrane aerated bioreactor. Journal of membrane science, 298(1), 110-116.
Meyer, C. E. (2015). Parameter Optimization for Start-up of a Simultaneous Nitrification/Denitrification Membrane Aerated Bioreactor (Doctoral dissertation).
Motlagh, A. R. A., LaPara, T. M., & Semmens, M. J. (2008). Ammonium removal in advective-flow membrane-aerated biofilm reactors (AF-MABRs). Journal of Membrane Science, 319(1), 76-81.
Motlagh, Ali R. Ahmadi, Vaughan R. Voller, and Michael J. Semmens.(2006). Advective flow through membrane-aerated biofilms: Modeling results." Journal of Membrane Science273.1-2:143-151.
Ni, B. J., & Yuan, Z. (2013). A model-based assessment of nitric oxide and nitrous oxide production in membrane-aerated autotrophic nitrogen removal biofilm systems. Journal of membrane science, 428, 163-171.
Nicolella, Cristiano, Prasert Pavasant, and Andrew G. Livingston. (2000). Substrate counterdiffusion and reaction in membrane-attached biofilms: mathematical analysis of rate limiting mechanisms. Chemical engineering science 55.8 1385-1398.
Nisola, G. M., Orata-Flor, J., Oh, S., Yoo, N., & Chung, W. J. (2013). Partial nitrification in a membrane-aerated biofilm reactor with composite PEBA/PVDF hollow fibers. Desalination and Water Treatment, 51(25-27), 5275-5282.
Ntwampe, Seteno KO, M. S. Sheldon, and H. Volschenk. (2008). Oxygen mass transfer for an immobilised biofilm of Phanerochaete chrysosporium in a membrane gradostat reactor. Brazilian Journal of Chemical Engineering 25.4 649-664.
Ohandja, D. G., & Stuckey, D. C. (2007). Biodegradation of PCE in a hybrid membrane aerated biofilm reactor. Journal of Environmental Engineering, 133(1), 20-27.
Ohandja, D. G., & Stuckey, D. C. (2010). Effect of perchloroethylene (PCE) and hydraulic shock loads on a membrane-aerated biofilm reactor (MABR) biodegrading PCE. Journal of chemical technology and biotechnology, 85(2), 294-301.
Pellicer-Nàcher, C., Domingo-Félez, C., Lackner, S., & Smets, B. F. (2013). Microbial activity catalyzes oxygen transfer in membrane-aerated nitritating biofilm reactors. Journal of membrane science, 446, 465-471.
Pellicer-Nàcher, C., Sun, S., Lackner, S., Terada, A., Schreiber, F., Zhou, Q., & Smets, B. F. (2010). Sequential aeration of membrane-aerated biofilm reactors for high-rate autotrophic nitrogen removal: experimental demonstration. Environmental science & technology, 44(19), 7628-7634.
Pellicer-Nàcher, C., Franck, S., Gülay, A., Ruscalleda, M., Terada, A., Al-Soud, W. A., ... & Smets, B. F. (2014). Sequentially aerated membrane biofilm reactors for autotrophic nitrogen removal: microbial community composition and dynamics. Microbial biotechnology, 7(1), 32-43.
Peng, L., Chen, X., Xu, Y., Liu, Y., Gao, S. H., & Ni, B. J. (2015). Biodegradation of pharmaceuticals in membrane aerated biofilm reactor for autotrophic nitrogen removal: A model-based evaluation. Journal of Membrane Science, 494, 39-47.
Phattaranawik, J., & Leiknes, T. (2009). Double-deck aerated biofilm membrane bioreactor with sludge control for municipal wastewater treatment. AIChE journal, 55(5), 1291-1297.
Picard, C., Logette, S., Schrotter, J. C., Aimar, P., & Remigy, J. C. (2012). Mass transfer in a membrane aerated biofilm. *Water research*, *46*(15), 4761-4769.
Plascencia-Jatomea, R., Almazán-Ruiz, F. J., Gómez, J., Rivero, E. P., Monroy, O., & González, I. (2015). Hydrodynamic study of a novel membrane aerated biofilm reactor (MABR): Tracer experiments and CFD simulation. *Chemical Engineering*

Science, *138*, 324-332.

Potvin, C. M., Long, Z., & Zhou, H. (2012). Removal of tetrabromobisphenol A by conventional activated sludge, submerged membrane and membrane aerated biofilm reactors. *Chemosphere*, *89*(10), 1183-1188.

Reij, Martine W., Jos TF Keurentjes, and Sybe Hartmans. (1998). Membrane bioreactors for waste gas treatment." Journal of Biotechnology 59.3: 155-167.

Richard T. Calculating the oxygen diffusion coefficient in water.
http://compost.css.cornell.edu/oxygen/oxygen.diff.water.html, 2005 (accessed 18 April 2018).

Rincon Bonilla, Mauricio, and Suresh K. Bhatia. (2013). Diffusion in pore networks: Effective self-diffusivity and the concept of tortuosity. The Journal of Physical Chemistry C 117(7), 3343-3357.

Rittmann, B. E. (1982). Comparative performance of biofilm reactor types. Biotechnology and bioengineering 24(6), 1341-1370.

Shanahan, J. W., & Semmens, M. J. (2015). Alkalinity and pH effects on nitrification in a membrane aerated bioreactor: An experimental and model analysis. *Water research*, *74*, 10-22.

Shanahan, John W., and Michael J. Semmens. (2004).Multipopulation model of membrane-aerated biofilms." Environmental science & technology 38(11),3176-3183.

Shaowei, H. U., Fenglin, Y. A. N. G., Cui, S. U. N., ZHANG, J., & Tonghua, W. A. N. G. (2008). Simultaneous removal of COD and nitrogen using a novel carbon-membrane aerated biofilm reactor. *Journal of Environmental Sciences*, *20*(2), 142-148.

Shechter, R. (2015). Energy efficiency and performance of a full scale membrane aerated biofilm reactor. *Proceedings of the Water Environment Federation*, 13, 5224-5228.

Simon, A., McDonald, J. A., Khan, S. J., Price, W. E., & Nghiem, L. D. (2013). Effects of caustic cleaning on pore size of nanofiltration membranes and their rejection of trace organic chemicals. Journal of membrane science, 447, 153-162.

Smits, Alexander J., and Jean-Paul Dussauge. (2006). Turbulent shear layers in supersonic flow. Springer Science & Business Media.

Stewart, P. S., Zhang, T., Xu, R., Pitts, B., Walters, M. C., Roe, F., & Moter, A. (2016). Reaction–diffusion theory explains hypoxia and heterogeneous growth within microbial biofilms associated with chronic infections. npj Biofilms and Microbiomes 2,16012.

Stricker, A. E., Lossing, H., Gibson, J. H., Hong, Y., & Urbanic, J. C. (2011). Pilot scale testing of a new configuration of the membrane aerated biofilm reactor (MABR) to treat high-strength industrial sewage. *Water Environment Research*, *83*(1), 3-14.

Sun, J., Dai, X., Liu, Y., Peng, L., & Ni, B. J. (2017). Sulfide removal and sulfur production in a membrane aerated biofilm reactor: Model evaluation. *Chemical Engineering Journal*, *309*, 454-462.

Sun, L., Wang, Z., Wei, X., Li, P., Zhang, H., Li, M., ... & Wang, S. (2015). Enhanced biological nitrogen and phosphorus removal using sequencing batch membrane-aerated biofilm reactor. *Chemical Engineering Science*, *135*, 559-565.

Syron, E., & Casey, E. (2008). Membrane-aerated biofilms for high rate biotreatment: performance appraisal, engineering principles, scale-up, and development requirements. *Environmental science & technology*, *42*(6), 1833-1844.

Syron, E., & Casey, E. (2008). Model-based comparative performance analysis of membrane aerated biofilm reactor configurations. *Biotechnology and bioengineering*, *99*(6), 1361-1373.

Syron, E., & Casey, E. (2012). Performance of a pilot scale Membrane Aerated Biofilm Reactor for the treatment of landfill leachate. *Procedia Engineering*, *44*, 2082-2084.

Syron, E., Kelly, H., & Casey, E. (2009). Studies on the effect of concentration of a self-inhibitory substrate on biofilm reaction rate under co-diffusion and counter-diffusion configurations. Journal of Membrane Science, 335(1), 76-82.

Syron, E., Semmens, M. J., & Casey, E. (2015). Performance analysis of a pilot-scale membrane aerated biofilm reactor for the treatment of landfill leachate. *Chemical Engineering Journal*, *273*, 120-129.

Syron, Eoin, and Eoin Casey. (2008). Model-based comparative performance analysis of membrane aerated biofilm reactor configurations." Biotechnology and bioengineering 99.6, 1361-1373.

Syron, Eoin, Hugh Kelly, and Eoin Casey. (2009). Studies on the effect of concentration of a self-inhibitory substrate on biofilm reaction rate under co-diffusion and counter-diffusion configurations." Journal of Membrane Science 335(1-2),76-82.

Tanase, C., Chirvase, A. A., Ungureanu, C., Caramihai, M., & Muntean, O. (2011). Study of double-substrate limited growth of Pseudomonas aeruginosa in aerobic bioprocess." Revue Roumaine Chemie 56, 1147.

Terada, A., Lackner, S., Kristensen, K., & Smets, B. F. (2010). Inoculum effects on community composition and nitritation performance of autotrophic nitrifying biofilm reactors with counter-diffusion geometry. Environmental microbiology, 12(10), 2858-2872.

Tian, H. L., Zhao, J. Y., Zhang, H. Y., Chi, C. Q., Li, B. A., & Wu, X. L. (2015). Bacterial community shift along with the changes in operational conditions in a membrane-aerated biofilm reactor. *Applied microbiology and biotechnology*, *99*(7), 3279-3290.

Tian, H., Yan, Y., Chen, Y., Wu, X., & Li, B. (2016). Process performance and bacterial community structure under increasing influent disturbances in a membrane-aerated biofilm reactor. *J Microbiol Biotechn*, *26*, 373-84.

Tian, H., Zhang, H., Li, P., Sun, L., Hou, F., & Li, B. (2015). Treatment of pharmaceutical wastewater for reuse by coupled membrane-aerated biofilm reactor (MABR) system. *RSC Advances*, *5*(85), 69829-69838.

Tong, K., Zhang, Y., Liu, G., Ye, Z., & Chu, P. K. (2013). Treatment of heavy oil wastewater by a conventional activated

sludge process coupled with an immobilized biological filter. International Biodeterioration & Biodegradation, 84, 65-71.

Vafajoo, L., & Pazoki, M. (2013). Model-based evaluations of operating parameters on CANON process in a membrane-aerated biofilm reactor. *Desalination and Water Treatment*, *51*(19-21), 4228-4234.
Villain, L., Meyer, L., Kroll, S., Beutel, S., & Scheper, T. (2008). Development of a Novel Membrane Aerated Hollow-Fiber Microbioreactor. *Biotechnology progress*, *24*(2), 367-371.
Wang, R., Terada, A., Lackner, S., Smets, B. F., Henze, M., Xia, S., & Zhao, J. (2009). Nitritation performance and biofilm development of co-and counter-diffusion biofilm reactors: modeling and experimental comparison. *Water research*, *43*(10), 2699-2709.
Wang, R., Xiao, F., Wang, Y., & Lewandowski, Z. (2016). Determining the optimal transmembrane gas pressure for nitrification in membrane-aerated biofilm reactors based on oxygen profile analysis." Applied microbiology and biotechnology 100(17), 7699-7711.
Wang, Y. K., Pan, X. R., Geng, Y. K., & Sheng, G. P. (2015). Simultaneous effective carbon and nitrogen removals and phosphorus recovery in an intermittently aerated membrane bioreactor integrated system. Scientific reports, 5, 16281.
Wanner, O., O. Debus, and P. Reichert. (1994). Modelling the spatial distribution and dynamics of a xylene-degrading microbial population in a membrane-bound biofilm." Water Science and Technology 29(10-11),243-251.
Wei, X., Li, B., Zhao, S., Qiang, C., Zhang, H., & Wang, S. (2012). COD and nitrogen removal in facilitated transfer membrane-aerated biofilm reactor (FT-MABR). *Journal of membrane science*, *389*, 257-264.
Wei, X., Li, B., Zhao, S., Wang, L., Zhang, H., Li, C., & Wang, S. (2012). Mixed pharmaceutical wastewater treatment by integrated membrane-aerated biofilm reactor (MABR) system–a pilot-scale study. *Bioresource technology*, *122*, 189-195.
Wu, J., & Zhang, Y. (2017). Evaluation of the impact of organic material on the anaerobic methane and ammonium removal in a membrane aerated biofilm reactor (MABR) based on the multispecies biofilm modeling. *Environmental Science and Pollution Research*, *24*(2), 1677-1685.
Xie, K., Xia, S., Song, J., Li, J., Qiu, L., Wang, J., & Zhang, S. (2014). The effect of salinity on membrane fouling characteristics in an intermittently aerated membrane bioreactor. *Journal of Chemistry*, *2014*.
Xudong, Z., Zongsheng, Z., Weijing, J., Jing, D., & Jing, J. (2010, June). Mathematical simulations of nitrogen removal via a partial nitrification-anaerobic ammonium oxidation in a membrane-aerated biofilm reactor. In *Mechanic Automation and Control Engineering (MACE), 2010 International Conference on* (pp. 2018-2025). IEEE.
Zhang, Tian C., and Paul L. Bishop. (1994). Density, porosity, and pore structure of biofilms.Water Research 28(11),2267-2277.
Zhao, Y., Liu, Z., Liu, F., & Li, Z. (2011). Cometabolic degradation of trichloroethylene in a hollow fiber membrane reactor with toluene as a substrate. *Journal of membrane science*, *372*(1), 322-330.
Zheng, M., & Liao, B. Q. (2014). A comparative study on thermomechanical pulping pressate treatment using thermophilic and mesophilic sequencing batch reactors. Environmental technology, 35(11), 1409-1417.
Zheng, M., & Liao, B. Q. (2016). Membrane aerated biofilm reactors for thermomechanical pulping pressate treatment. International Journal of Chemical Reactor Engineering, 14(5), 1017-1024.